September 20, 2010
RECAPP-HRI-2010-009

Discrimination of low missing energy look-alikes at the LHC

Kirtiman Ghosh*, Satyanarayan Mukhopadhyay†, Biswarup Mukhopadhyaya‡

Regional Centre for Accelerator-based Particle Physics
Harish-Chandra Research Institute
Chhatnag Road, Jhusi
Allahabad - 211 019, India

Abstract

The problem of discriminating possible scenarios of TeV scale new physics with large missing energy signature at the Large Hadron Collider (LHC) has received some attention in the recent past. We consider the complementary, and yet unexplored, case of theories predicting much softer missing energy spectra. As there is enough scope for such models to fake each other by having similar final states at the LHC, we have outlined a systematic method based on a combination of different kinematic features which can be used to distinguish among different possibilities. These features often trace back to the underlying mass spectrum and the spins of the new particles present in these models. As examples of "low missing energy look-alikes", we consider Supersymmetry with R-parity violation, Universal Extra Dimensions with both KK-parity conserved and KK-parity violated and the Littlest Higgs model with T-parity violated by the Wess-Zumino-Witten anomaly term. Through detailed Monte Carlo analysis of the four and higher lepton final states predicted by these models, we show that the models in their minimal forms may be distinguished at the LHC, while non-minimal variations can always leave scope for further confusion. We find that, for strongly interacting new particle mass-scale ~ 600 GeV (1 TeV), the simplest versions of the different theories can be discriminated at the LHC running at $\sqrt{s} = 14$ TeV within an integrated luminosity of 5 (30) fb^{-1}.

*kirtiman@hri.res.in
†satya@hri.res.in
‡biswarup@hri.res.in

1 Introduction

The Large Hadron Collider (LHC) marks the beginning of an era where physics at the TeV scale can be probed at an unprecedented level. One important goal of such investigations is to see whether the standard model (SM) of elementary particles is embedded within a set of new laws which make their presence felt at the TeV scale. Several proposals of such new physics (NP) have been put forward, with motivations ranging from the naturalness problem of the Higgs mass to solving the dark matter puzzle.

Quite a few of such models systematically predict a host of new particles occurring in correspondence with those present in the SM. In addition, the need to accommodate an invisible, weakly interacting particle qualifying as a dark matter candidate often invites the imposition of a Z_2 symmetry on the theory, which renders the lightest of the new particles stable. This leads to the prediction of large missing transverse energy (MET) at the LHC, due to the cascades of new particles ending up in the massive stable particle that eludes the detectors. Such MET (together with energetic jets, leptons etc.) goes a long way in making such new physics signals conspicuous. Even then, however, one has to worry about distinguishing among different theoretical scenarios, once some excess over SM backgrounds is noticed. Thus one has the task of using the LHC data to differentiate among models like supersymmetry (SUSY), universal extra dimensions (UED) and littlest Higgs with T-parity (LHT), all of which are relevant at the TeV scale. With the SM particles supplemented with new, more massive ones having the same gauge quantum numbers (with only spins differing in the case of SUSY) in all cases, their signals are largely similar. The consequent problem of finding out the model behind a given set of signatures is often dubbed as the LHC inverse problem. The name was coined when it was shown first in the context of SUSY [1] that different choices of parameters within SUSY lead to quantitatively similar LHC signals. The efforts towards distinction were subsequently extended to the aforementioned different scenarios with large missing energy signature at the LHC [2, 3, 4].

Though the scenarios predicting MET signals are attractive from the viewpoint of explaining the dark matter content of the universe, and they also satisfy the electroweak precision constraints while keeping the new particle spectrum 'natural', the discrete symmetry ensuring the stability of the weakly interacting massive particles is almost always introduced in an *ad hoc* manner. For example, it is well-known that the superpotential of the minimal SUSY standard model (MSSM) can include terms which violate the conventionally imposed R-parity, defined as $R = (-)^{(3B+L+2S)}$. If SUSY exists, the violation of R-parity cannot therefore be ruled out. Similarly, boundary terms in UED can violate the Kaluza-Klein parity usually held sacrosanct, and T-parity in LHT can be broken by the so-called Wess-Zumino-Witten anomaly term. While one is denied the simplest way of having a dark matter candidate when the Z_2 symmetry is broken, these are perfectly viable scenarios phenomenologically, perhaps with some alternative dark matter candidate(s). In SUSY, for example, the axino or the gravitino can serve this purpose even if R-parity is broken. And, most importantly, the different scenarios with broken Z_2 are as amenable to confusion as their Z_2-preserving counterparts, as far as signals at the LHC are concerned. The mostly sought-after final states (such as jets + dileptons) are expected from all of these scenarios, various kinematical features are of similar appearance, and in none of the cases does one have the MET tag for ready recognition, in clear contrast to scenarios with unbroken Z_2.

Side by side with the problem of large missing energy look-alike models, the disentanglement of 'low missing energy look-alikes' is thus an equally challenging issue, on which not much work has been done yet. Some criteria for distinction among this class of look-alikes are developed in this paper. Specifically, we consider four possible scenarios of NP with low missing energy signature:

1. Supersymmetry with R-parity violation (SUSY-RPV)
2. Minimal universal extra dimensions (mUED) with KK-parity conserved (UED-KKC)
3. Minimal universal extra dimensions with KK-parity violated (UED-KKV)
4. Littlest Higgs model with T-parity violated by the Wess-Zumino-Witten anomaly term (LHT-TPV).

It should be noted that UED-KKC is also included in this study. This is because, as will be seen in the following sections, the peculiar features of the mUED spectrum (namely, a large degree of degeneracy) often leads to the lightest stable particle carrying very low transverse momentum. In addition, one often also has nearly back-to-back emission of the invisible particle pair. Consequently, the MET spectrum is rather soft over a large region of the parameter space, and the signals can be of similar nature as those of Z_2-violating scenarios. Hence we would like to emphasize that mUED with KK-parity conserved is a scenario which can be easily distinguished by its much softer MET spectrum from other models predicting a massive stable particle (like SUSY with R-parity), but might actually be confused with the other Z_2-violating scenarios.

It is well-known that signals containing leptons have relatively less SM backgrounds compared to events with fully hadronic final states. We therefore focus on possible leptonic channels in the various models under consideration. One has to note, however, that it is difficult to devise model-independent cuts such that the SM backgrounds are reduced while keeping a significant fraction of the signal events intact for all the models. For example, strong cuts on the transverse momenta of the leptons cannot be applied in case of mUED as the leptons there are very soft in general, owing to the almost degenerate spectrum of the Kaluza-Klein excitations. This makes it difficult to reduce the SM backgrounds in the single lepton and opposite-sign dilepton channels (which have rather large irreducible backgrounds from $W+$ jets and $t\bar{t}+$ jets respectively). Although same-sign dilepton and trilepton channels have relatively lower rates within the SM, they are not very suitable for the purpose of distinguishing between the above models. The main reason for this is that many otherwise conspicuous invariant mass peaks cannot be reconstructed in these channels. These invariant mass peaks, however, are very helpful in classifying the models. In addition, since one is now looking at situations where the NP signals are *not* accompanied by large MET, rising above the SM backgrounds is a relatively harder task which is accomplished better with a larger multiplicity of leptons. Keeping this mind, here we have tried to develop a procedure of model discrimination, depending on four-and higher-lepton signals as far as possible.

The four-lepton channel is viable in all the four models mentioned above, and such events can be used to extract out several qualitative differences among the models, including the

presence or absence of mass peaks. Therefore, our study largely focuses on the four-lepton channel. Furthermore, since most cascades start with the production of strongly interacting heavier particles in these new theories, as we can be seen from the appendix, generically we can obtain at least two hadronic jets in the signal. Apart from the four-lepton channel, we also use the presence (or absence) of signals with even higher lepton multiplicity as a discriminating feature. It is of course true that these methods of discrimination can often be applied only after sufficient luminosity has been accumulated. In this sense, our study differs from that of [2], where the inverse problem was considered not only for models with a very large MET signal, but also at a modest luminosity of $200\,\mathrm{pb}^{-1}$ only.

The paper is organized as follows. The choice of relevant parameters in the various models considered and our general strategy and methods adopted in event generation at the LHC are summarised in section 2. We use this strategy to show some predictions in section 3 to convince the reader that the different scenarios indeed fake each other considerably at the LHC. Section 4 is devoted to a detailed study of kinematics of four-lepton final states, whereby a significant set of distinction criteria are established. In section 5, we discuss the usefulness of the channel with five or more leptons. Some scenarios over and above those covered here in details are qualitatively commented upon in section 6. We summarise and conclude in section 7. Finally, as a useful reference for the reader, we outline the main features of the low-missing energy look-alike models and the possible cascades through which four and higher-lepton signals can arise in those contexts, in an Appendix.

2 Multilepton final states: signal and background processes

2.1 Event generation and event selection criteria

Before we establish that the models mentioned in the introduction (and described in the Appendix) all qualify as look-alikes with low MET, and suggest strategies for their discrimination through multilepton channels, we need to standardise our computation of event rates in these channels. With this in view, we outline here the methodology adopted in our simulation, and the cuts imposed for reducing the SM backgrounds. The predicted rates of events for some benchmark points, after the cuts are employed, are presented at the end of this section.

As the production cross-section for strongly interacting particles is high at the LHC, we start with the production of these heavier 'partners' (having different spins for SUSY-RPV, and same spins in the remaining cases) of quarks and gluons at the initial parton level $2 \to 2$ scattering. Though in principle there are contributions to the multilepton final states from electroweak processes as well, they are subleading, and are left out in our estimate. In this sense, our estimates of the total cross-sections in various channels, are in fact lower bounds. Also, the observations made by us subsequently on final state kinematics are unaltered upon the inclusion of these subleading effects.

For our simulation of signal processes, in case of SUSY-RPV, we have used PYTHIA 6.421 [5] for simulating both the production of strongly interacting particles and their subsequent decays. Since the values of the L-violating couplings that we have taken are very

small, they do not affect the renormalisation group running of mass parameters from high to low scale [6]. Therefore, The SUSY spectrum is generated with SuSpect 2.41 [7]. For UED, while the production is once again simulated with the help of PYTHIA, both KK-parity conserving and KK-parity violating decay branching fractions are calculated in CalcHEP 2.5 [8] using the model file written by [9] and then passed on to PYTHIA via the SUSY/BSM Les Houches Accord (SLHA) (v1.13) [10]. For UED-KKV, we have implemented the relevant KK-parity violating decay modes in CalcHEP. Finally, for LHT with T-violation the initial parton level hard-scattering matrix elements were calculated and the events generated with the help of CalcHEP. These events, along with the relevant masses, quantum numbers and decay branching fractions were passed on PYTHIA with the help of the SLHA interface for their subsequent analysis. In all cases, showering, hadronization, initial and final state radiations from QED and QCD and multiple interactions are fully included while using PYTHIA.

To simulate the dominant SM backgrounds, events for the processes ZZ and $t\bar{t}$ were generated with PYTHIA. Backgrounds from $t\bar{t}Z$ have been simulated with the generator ALPGEN [11], and the unweighted event samples have been passed onto PYTHIA for the subsequent analysis.

We have used the leading order CTEQ6L1 [12] parton distribution functions. Specifically, for PYTHIA, the Les Houches Accord Parton Density Function (LHAPDF) [13] interface has been used. The QCD factorization and renormalization scales are in general kept fixed at the sum of masses of the particles which are produced in the initial parton level hard scattering process. If we decrease the QCD scales by a factor of two, the cross-section can increase by about 30%.

While the signal primarily used in our analysis is $4l + nj + \not{E}_T$ ($n \geq 2$), we have also considered events with five or more number of leptons in section 5. No restriction was made initially on the signs and flavours of the leptons. As we shall see subsequently, the 'total charge of leptons' can be used as a useful discriminator at a later stage of the analysis.

The different ways in which multilepton signals can arise in the various models under consideration have been described in the appendix. The principal backgrounds to the $4l + nj + \not{E}_T$ channel ($n \geq 2$) are ZZ/γ^*, $t\bar{t}$ and $t\bar{t}Z/\gamma^*$. Although in case of ZZ (where the two associated jets can come from ISR and FSR), there is no real source of MET if we demand a $4l$ signal (i.e., both the Z's have to decay leptonically), jet energy mismeasurement can give rise to some amount of fake MET.

The following basic selection cuts were applied for both the signal and the background [14, 15]:

Lepton selection:

- $p_T > 10$ GeV and $|\eta_\ell| < 2.5$, where p_T is the transverse momentum and η_ℓ is the pseudorapidity of the lepton (electron or muon).
- **Lepton-lepton separation:** $\Delta R_{\ell\ell} \geq 0.2$, where $\Delta R = \sqrt{(\Delta\eta)^2 + (\Delta\phi)^2}$ is the separation in the pseudorapidity–azimuthal angle plane.
- **Lepton-jet separation:** $\Delta R_{\ell j} \geq 0.4$ for all jets with $E_T > 20$ GeV.
- The total energy deposit from all *hadronic activity* within a cone of $\Delta R \leq 0.2$ around the lepton axis should be ≤ 10 GeV.

Jet selection:

- Jets are formed with the help of PYCELL, the inbuilt cluster routine in PYTHIA. The minimum E_T of a jet is taken to be 20 GeV, and we also require $|\eta_j| < 2.5$.

We have approximated the detector resolution effects by smearing the energies (transverse momenta) with Gaussian functions [14, 15]. The different contributions to the resolution error have been added in quadrature.

- **Electron energy resolution:**

$$\frac{\sigma(E)}{E} = \frac{a}{\sqrt{E}} \oplus b \oplus \frac{c}{E}, \tag{1}$$

where

$$(a, b, c) = \begin{cases} (0.030\ \text{GeV}^{1/2},\ 0.005,\ 0.2\ \text{GeV}), & |\eta| < 1.5, \\ (0.055\ \text{GeV}^{1/2},\ 0.005,\ 0.6\ \text{GeV}), & 1.5 < |\eta| < 2.5. \end{cases} \tag{2}$$

- **Muon p_T resolution:**

$$\frac{\sigma(p_T)}{p_T} = \begin{cases} a, & p_T < 100\ \text{GeV}, \\ a + b \log \dfrac{p_T}{100\ \text{GeV}}, & p_T > 100\ \text{GeV}, \end{cases} \tag{3}$$

with

$$(a, b) = \begin{cases} (0.008,\ 0.037), & |\eta| < 1.5, \\ (0.020,\ 0.050), & 1.5 < |\eta| < 2.5. \end{cases} \tag{4}$$

- **Jet energy resolution:**

$$\frac{\sigma(E_T)}{E_T} = \frac{a}{\sqrt{E_T}}, \tag{5}$$

with $a = 0.5\ \text{GeV}^{1/2}$, the default value used in PYCELL.

Under realistic conditions, one would of course have to deal with aspects of misidentification of leptons and jet energy mismeasurement.

Note that, in addition to the basic cuts discussed above and the further cuts on the lepton p_T's described in the next sub-section, we also have used a cut on the invariant mass of the opposite sign (OS) lepton pairs formed out of the four-leptons. We have demanded that $M_{l^+l^-} > 10$ GeV for all the OS lepton pairs. This cut helps us in reducing backgrounds coming from γ^* produced in association with a Z-boson or top quark pairs. *We shall collectively refer to the basic isolation cuts and this cut on dilepton invariant masses as* **Cut-1**.

2.2 Numerical results for four-lepton events

Two benchmark points have been chosen for each of the look-alike models and it is seen that the four and higher lepton signals can rise well above SM backgrounds, thus forming the basis of further kinematic analyses. In order to show that our analysis is independent of the mass-scale of new physics involved, we have chosen two benchmark points with different mass spectra. Also, we should emphasize here that in the subsequent analysis we shall be using kinematic features of the final states predicted by the different models which are largely independent of the choice of parameters. This is precisely why we take two different benchmark points and demonstrate that the essential qualitative distinctions between the models do not change as we go from one point to another. *Thus our conclusions reflect distinction among the various low-MET models as a whole, and do not pertain to specific benchmark points.* The relevant parameters of these models and their values at the benchmark points are described below. For details about the models, we refer the reader to the Appendix.

For SUSY-RPV, we have worked in the minimal supergravity (mSUGRA) framework. This is done just with an economy of free parameters in view, and it does not affect our general conclusions. In this framework, the MSSM mass spectrum at the weak scale is determined by five free parameters. Among them the universal scalar (m_0) and gaugino masses ($m_{1/2}$) and the universal soft-breaking trilinear scalar interaction (A_0) are specified as boundary conditions at a high scale (in this case the scale of gauge coupling unification), while the ratio of the vacuum expectation values of the two Higgs doublets ($\tan\beta$) and the sign of the Higgsino mass parameter ($\mathrm{sgn}(\mu)$) as defined in eqn. A-1 are specified at the electroweak scale. In our analysis the electroweak scale has been fixed at $\sqrt{m_{\tilde{t}_1} m_{\tilde{t}_2}}$, where $\tilde{t}_1$ and $\tilde{t}_2$ are the two mass eigenstates of the top squarks respectively.

In case of the minimal universal extra dimension (mUED) model with conserved Kalutza-Klein (KK) parity (UED-KKC), the essential parameters determining the mass spectrum are the radius of compactification (R) and the ultra-violet cut-off scale of the theory (Λ). Although in mUED with KK-parity violated (UED-KKV) we have an additional parameter h, for small values of this parameter, R and Λ once again primarily determine the mass spectrum.

In the Littlest Higgs model with T-parity violation (LHT-TPV), the new T-odd quark and gauge boson masses are determined by two parameters: f and κ_q (see Appendix for their precise definitions). Apart from that, an additional parameter κ_l appears in the T-odd lepton sector, which we have fixed to be equal to 1.0 throughout our study.

The choice of parameters for the different models are as follows:

1. **Point A:**

   - *SUSY-RPV*: $m_0 = 100$ GeV, $m_{1/2} = 250$ GeV, $\tan\beta = 10$, $A_0 = -100$ and $\mathrm{sgn}(\mu) > 0$. The RPV coupling taken is $\lambda_{122} = 10^{-3}$. With these choices, we find the sparticle masses relevant to our study as (all in GeV) $m_{\tilde{g}} = 606$, $m_{\tilde{\chi_1}^0} = 97$, $m_{\tilde{\chi_1}^\pm} = 180$, $m_{\tilde{d_L}} = 568$, $m_{\tilde{t}} = 399$, $m_{\tilde{e_L}} = 202$, $m_{\tilde{\nu_{eL}}} = 186$.
   - *LHT-TPV*: $f = 1500$ GeV, $k_q = 0.285$. With these choices, we find the T-odd particle masses relevant to our study as (all in GeV) $u_H = 603$, $d_H = 605$, $A_H = 230$, $W_H = Z_H = 977$.

- *UED-KKC*: $R^{-1} = 475$ GeV and $\Lambda = 20R^{-1}$. With these choices of UED-KKC parameters, the masses of relevant KK-particles are given by (all in GeV), $m_{g_1} = 609$, $m_{Q_1} = 568$, $m_{Z_1} = 509$, $m_{W_1} = 509$, $m_{l_1} = 489$ and $m_{\gamma_1} = 476$.
- *UED-KKV*: For UED-KKV, the values of R^{-1} and Λ are chosen to be same as in the case of UED-KKC. The value of the KK-parity violating parameter h is set to 0.001.

2. **Point B:**

- *SUSY-RPV*: $m_0 = 100$ GeV, $m_{1/2} = 435$ GeV, $\tan\beta = 5$, $A_0 = 0$ and $\mathrm{sgn}(\mu) > 0$. The RPV coupling taken is $\lambda_{122} = 10^{-3}$. With these choices, we find the sparticle masses relevant to our study as (all in GeV) $m_{\tilde{g}} = 1009$, $m_{\tilde{\chi_1}^0} = 176$, $m_{\tilde{\chi_1}^\pm} = 331$, $m_{\tilde{d_L}} = 927$, $m_{\tilde{t}} = 695$, $m_{\tilde{e_L}} = 309$, $m_{\tilde{\nu_{eL}}} = 300$.
- *LHT-TPV*: $f = 2375$ GeV, $k_q = 0.285$. With these choices, we find the T-odd particle masses relevant to our study as (all in GeV) $u_H = 956$, $d_H = 957$, $A_H = 368$, $W_H = Z_H = 1549$.
- *UED-KKC*: $R^{-1} = 800$ GeV and $\Lambda = 20R^{-1}$. With these choices of UED-KKC parameters, the masses of relevant KK-particles are given by (all in GeV), $m_{g_1} = 1025$, $m_{Q_1} = 956$, $m_{Z_1} = 851$, $m_{W_1} = 851$, $m_{l_1} = 824$ and $m_{\gamma_1} = 800$.
- *UED-KKV*: For UED-KKV, the values of R^{-1} and Λ are chosen to be same as in the case of UED-KKC. The value of the KK-parity violating parameter h is set to 0.001.

For LHT-TPV, UED-KKC and UED-KKV the Higgs mass has been fixed at 120 GeV. The top quark mass has been taken as 175 GeV in our study. In LHT-TPV, the value of κ_l has been kept fixed at 1. The choices of f and κ_q have been made in order to match the mass scale of the strongly interacting particles in LHT with those of the other models (these particles are predominantly produced in the initial hard scattering at the LHC). We should note here that this could have also been achieved with other different choices of these parameters, and we have remarked about their implication in section 4.2.

Table 1 shows the signal and SM background cross-sections for the $4l+ \geq 2j + \not{E}_T$ channel at LHC running with $\sqrt{s} = 14$ TeV after Cut-1 and additional cuts on lepton p_T's. The signal cross-sections are shown for the two above different choices of parameters in each model. On the whole, it is evident from the table that our event selection criteria assure us of enough background-free events in each case. The backgrounds look somewhat challenging for LHT-TPV for benchmark point B. However, one still can achieve a significance (defined as $S/\sqrt{B}$, S and B being respectively the number of signal and background events) of 5σ with an integrated luminosity of 30 fb^{-1}. For point A, $5\,\mathrm{fb}^{-1}$ is likely to be sufficient for raising the signal way above the backgrounds, and attempting discrimination among various theoretical scenarios via kinematical analysis.

We also show the sensitivity of the signals of the different scenarios to gradually tightened p_T cuts on the leptons. Clearly, the close degeneracy of the spectrum in UED-KKC makes the leptons softer. Thus the signal events fall with stronger cuts imposed on the relatively softer leptons. Although such cuts applied during the offline analysis can be useful in discriminating

Point A				
p_T^l Cuts (GeV)	SUSY-RPV (fb)	LHT-TPV (fb)	UED-KKC (fb)	UED-KKV (fb)
(10,10,10,10)	9450.91	21.09	163.36	14008.93
(20,10,10,10)	9447.87	21.09	129.29	13990.97
(20,20,10,10)	**9354.09**	**20.96**	**75.13**	**13819.24**
(20,20,20,10)	8486.90	19.66	30.73	11781.96
(20,20,20,20)	5013.02	12.90	7.16	7697.5
Point B				
(10,10,10,10)	756.00	1.71	26.24	872.94
(20,10,10,10)	756.00	1.71	25.83	872.74
(20,20,10,10)	**755.22**	**1.71**	**22.81**	**868.90**
(20,20,20,10)	736.43	1.66	14.73	804.96
(20,20,20,20)	555.70	1.22	4.77	520.27
SM Backgrounds				
	ZZ/γ^*	$t\bar{t}$	$t\bar{t}Z/\gamma^*$	Total
(10,10,10,10)	2.18	0.51	0.87	3.56
(20,10,10,10)	2.18	0.51	0.87	3.56
(20,20,10,10)	**2.17**	**0.43**	**0.87**	**3.47**
(20,20,20,10)	2.06	0.17	0.79	3.02
(20,20,20,20)	1.42	0.09	0.55	2.06

Table 1: Cut-flow table showing the change in $4l+ \geq 2j + \not{E}_T$ cross-section as we gradually increase the cuts on the lepton p_T. The p_T cuts shown within the brackets are ($p_T^{l_1}$, $p_T^{l_2}$, $p_T^{l_3}$, $p_T^{l_4}$) where l_1, l_2, l_3 and l_4 are the four leptons ordered according to their p_T's. The signal (point A and point B) and the SM background cross-sections quoted are for $\sqrt{s} = 14$ TeV. For all our subsequent analysis of four-lepton events, we have used the (20,20,10,10) cut. *We shall refer to this cut, applied in addition to Cut-1, as* **Cut-2**.

the UED-KKC scenario from the rest, one has to use this yardstick with caution. This is because the situation can change with different values of the UED parameters R^{-1} and Λ (as can be seen from point B). While they also change the KK excitation masses together with changing the mass-splitting, the estimate of masses from data for UED is not reliable, for reasons to be discussed in the next section. We therefore suggest some kinematical criteria that bypass this caveat.

3 On what ground are the models look-alikes?

In addition to the fact that all the suggested models have appreciable cross-section in the four lepton channel (and also in various other channels that we are not considering for model-discrimination for reasons described in the introduction), in order to ascertain that these models are indeed look-alikes, we first show that certain kinematic distributions, like

MET or effective mass have very similar features in these scenarios of new physics. To begin with, we note that with similar masses of the strongly interacting new particles (squarks and gluinos for SUSY-RPV, q_1 and g_1 for the two variants of UED, and q_H for LHT-TPV), the MET distributions look similar.

The missing transverse energy in an event is given by

$$\not{E}_T = \sqrt{\left(\sum p_x\right)^2 + \left(\sum p_y\right)^2}. \tag{6}$$

Here the sum goes over all the isolated leptons, the jets, as well as the 'unclustered' energy deposits.

The MET distributions for the four scenarios under study are shown in Figure 1. The similarity of the MET distributions is obvious in all the four cases, including UED-KKC. For UED-KKC, as mentioned before, the reason behind this is the close degeneracy of the spectra. As a result, in this model the two γ_1's produced at the end of the cascades on the two sides have little transverse momentum, and quite often they are also back-to-back in the transverse plane. Consequently, the net MET is considerably reduced, in spite of the γ_1 being a massive particle. Thus UED-KKC is as much of a look-alike with SUSY-RPV and LHT-TPV as UED-KKV.

The confusion among the look-alikes from MET distributions is expected to be more for similar values of the masses of the strongly interacting new particles. Since the direct measurement of mass at LHC is not easy, a measured quantity that often bears the stamp of these masses is the so-called effective mass. It is defined as the scalar sum of the transverse momenta of the isolated leptons and jets and the missing transverse energy,

$$M_{eff} = \sum p_T^{jets} + \sum p_T^{leptons} + \not{E}_T, \tag{7}$$

Note that although usually M_{eff} carries the information about the mass scale of the particles produced in the initial parton level hard scattering, this is not true in all cases. Specifically, it is well-known that for a mass spectrum which is very closely spaced, M_{eff} largely underestimates the relevant mass-scale, the reason being very similar to that for the MET distribution being low in UED-KKC.

If an excess is seen in the $4l+nj+\not{E}_T$ $(n \geq 2)$ channel, fingers can be pointed at the several models mentioned before. Figure 1 is an example where the MET distributions show similar behaviour when the strongly interacting heavy particles in all of the four aforementioned models under consideration have similar masses. We thus conclude that all the four models clearly qualify as missing energy look-alikes. The minor differences that exist are difficult to use as discriminators, as these can be masked by features of the detector as well as systematic errors. In Figure 2, we also present the M_{eff} distributions for all these models, for the same 'mass scale' of ~ 600 GeV (1000 GeV) for point A (point B). One finds that all the models except UED-KKC have a peak in the M_{eff} distribution at around twice the mass-scale (i.e., ~ 1200 GeV for point A). For point A in UED-KKC, the distribution peaks at around 300 GeV. Similar features are also observed for point B.

This fact, if correlated with the total cross-section, can perhaps be used to single out the UED-KKC model from the remaining three. However, one can still vary the excited quark

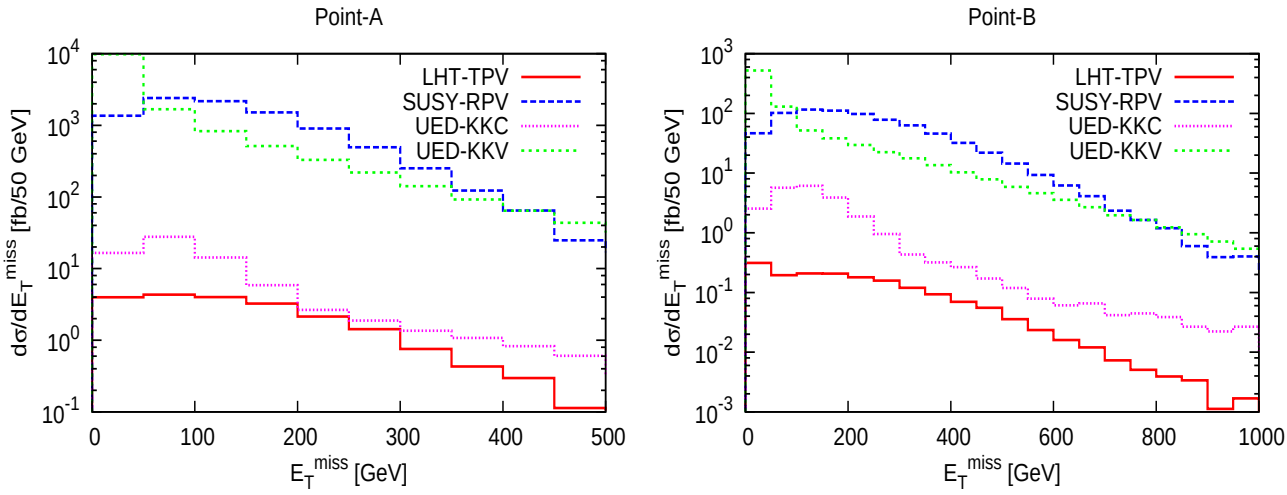

Figure 1: Missing E_T distribution in various models for point A (left figure) and point B (right figure), at $\sqrt{s} = 14$ TeV after Cut-2.

and gluon masses in UED-KKC to match both the MET distributions for other models with a 600 GeV mass-scale. In order for this to happen, however, R^{-1} has to be as large as about 3 TeV. This would not only lead to very low total cross-section but also imply a scenario that is ruled out due to overclosure of the universe through γ_1.

However, while similar MET distribution but much softer M_{eff} distribution can single out UED-KKC, similar distributions in both variables but very low cross-sections can be noticed in special situations in the other models as well. For example, one can have RPV SUSY with both the λ-and λ'-type interactions, with the later being of larger value, thus suppressing the decay of the lightest neutralino into two leptons. In such a case, with $m_{\tilde{q}} \simeq m_{\tilde{g}} \simeq 600$ GeV, the MET as well as M_{eff}-distributions will be very similar as earlier, but the cross-section may be down by a large factor.

The above example shows that there is a pitfall in using total rate as a discriminant. Keeping this in view, we choose our benchmark points with similar masses for all the models but look for other kinematical features where the differences show up.

4 Analysis of $4l$ events

4.1 Four-lepton invariant mass distribution: two classes

In the table containing rates of four-lepton final states, we have allowed all the leptons to be of either charge. While we keep open the option of having all charge combinations, in this and the next two subsections we concentrate on those events where one has two positive and two negatively charged leptons. The issue of 'total charge of the set of leptons' and its usefulness in model discrimination is taken up section 5.4.

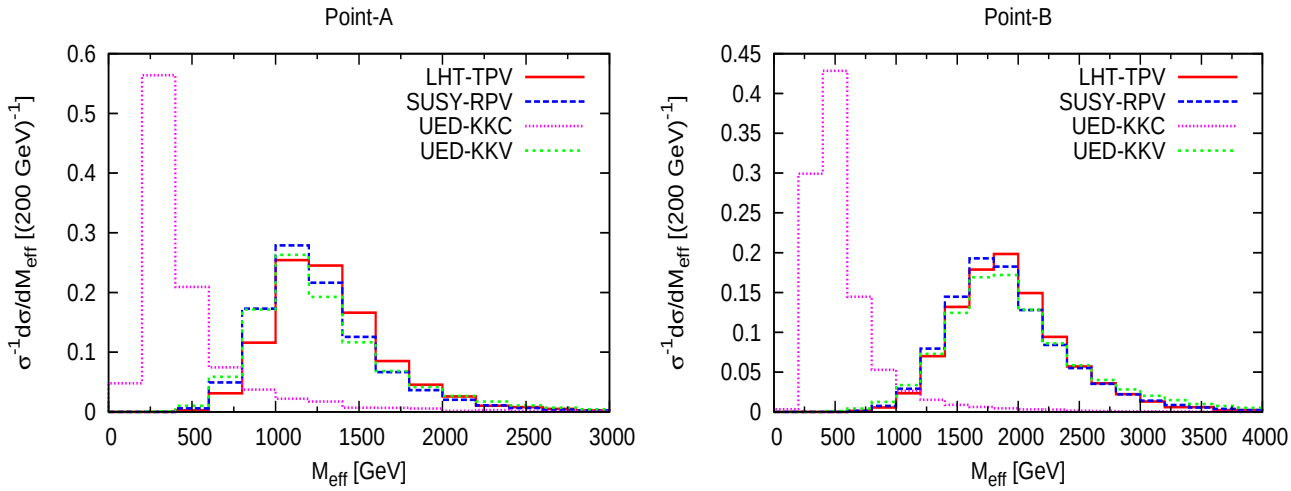

Figure 2: Normalized effective mass distribution in various models for point A (left figure) and point B (right figure), at $\sqrt{s} = 14$ TeV after Cut-2.

For the $4l + nj + \not{E}_T$ channel (with $n \geq 2$), the first distribution that we look into is that of the four-lepton invariant mass (M_{4l}). From Figure 3 we can see that, based on the M_{4l} distribution the models can be classified into two categories, 1) those with a peak in the M_{4l} distribution and 2) those without any such peak.

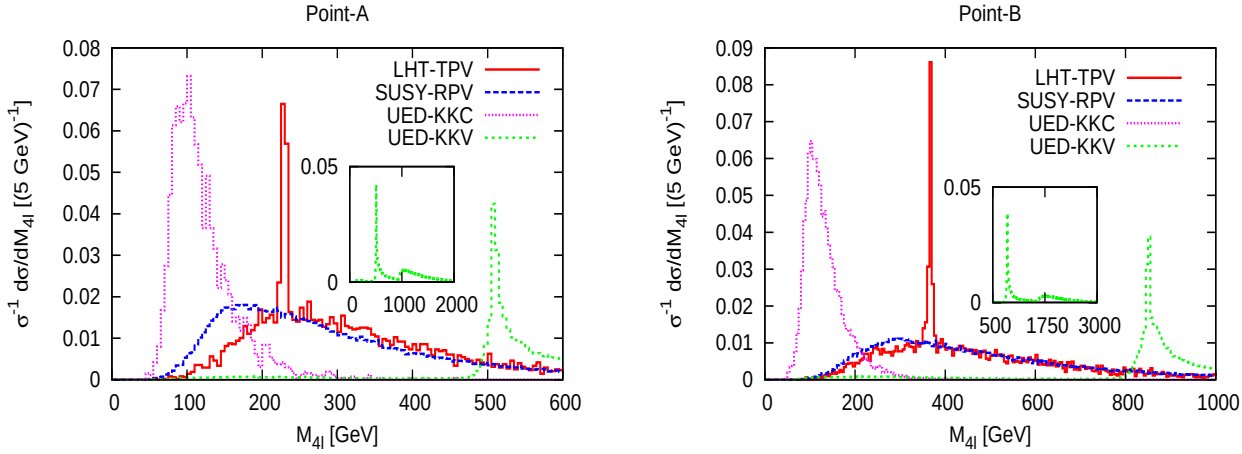

Figure 3: Normalized invariant mass distribution of four leptons (M_{4l}) in the different models for point A (left figure) and point B (right figure), at $\sqrt{s} = 14$ TeV. The insets show the full range of M_{4l} for UED-KKV. The distributions have been plotted after Cut-2.

In SUSY-RPV, there is no single bosonic particle decaying, via cascade, to four leptons. Hence, no invariant mass peak is expected in this model and the M_{4l} distribution has a very broad shape, as we see in Figure 3. As discussed earlier, in the example taken, the four leptons here come from the RPV decays of the neutralino and the RPC decays of the chargino.

Similarly, in UED-KKC the four leptons come from the two cascade decay chains and not from a single particle. In this case, the decay of a Z_1 gives two leptons of opposite charge and same flavour in each chain. Note that the range in which M_{4l} takes values for UED-KKC is rather restricted, as can be seen in Figure 3. We can understand this in the following manner. Let us denote the four-momenta of the two leptons coming from one chain by p_1 and p_2, and those of the other two from the second chain by p_3 and p_4. Then, an approximate upper bound on M_{4l} can be obtained as follows:

$$\begin{aligned} M_{4l}^2 &= (p_1+p_2+p_3+p_4)^2 \\ &= (p_1+p_2)^2+(p_3+p_4)^2+2(p_1+p_2).(p_3+p_4) \end{aligned} \tag{8}$$

Now,

$$(p_1+p_2)^2 \leq \frac{(M_{Z_1}^2-M_{L_1}^2)(M_{L_1}^2-M_{\gamma_1}^2)}{M_{L_1}^2} \tag{9}$$

A similar bound is also applicable to $(p_3+p_4)^2$. Finally, we can approximate

$$2p_1.p_3 = 2(E_1E_3-\vec{p_1}.\vec{p_3}) \simeq 2E_1E_3(1-cos\theta_{13}) \leq 4E_1E_3 \tag{10}$$

Here θ_{13} is the angle between $\vec{p_1}$ and $\vec{p_3}$. Hence, we can finally approximate the upper bound on M_{4l} for UED-KKC as

$$M_{4l} \leq \sqrt{2\frac{(M_{Z_1}^2-M_{L_1}^2)(M_{L_1}^2-M_{\gamma_1}^2)}{M_{L_1}^2}+4[E_1E_3+E_1E_4+E_2E_3+E_2E_4]} \tag{11}$$

The first term within the square-root has the numerical value of about 2400 GeV^2 for point A in UED-KKC. Because of the unknown boost of the partonic centre of mass frame, we cannot put any definite upper bound on the p_T's of Z_1 and L_1, and therefore the maximum possible values of the lepton energies E_i are also undetermined. Still, as very little energy is available at the rest frame of the decaying KK-excitations (once again because of low mass-splittings), E_i cannot be very large. This is the reason we expect M_{4l} for UED-KKC to take values in a somewhat restricted range.

For UED-KKV, we observe a very sharp peak in the M_{4l} distribution around $\sim$ 510 GeV (850 GeV) which is the mass of Z_1 for point A (point B). The four leptons in this case come from the cascade decay of a Z_1 to a lepton pair and a γ_1 followed by the KKV decay of the γ_1 to another pair of leptons. There is of course a long tail in the M_{4l} distribution here coming from the cases where all four of the leptons do not come from the decay of a single Z_1. For example, they can come from the leptonic decay of the two γ_1's via KK-parity violating interactions. We demonstrate this full range in the insets of Figure 3. It is, however, important to note that, in these cases, M_{4l} mostly exceeds M_{γ_1} when two of

the leptons come from γ_1 decay and the two others come from the cascade. On the other hand, the invariant mass is greater than $2M_{\gamma_1}$ when the four leptons come from the decay of two γ_1's. This is why we observe an excess after around 1 TeV (1.6 TeV) for point A (point B) in the insets of Figure 3. As long as we have a γ_1 LKP with KK-parity violating interactions, this very clear peak, followed by a hump, observable in the M_{4l} distribution is a very important feature of UED-KKV.

Finally in LHT-TPV, we see in Figure 3 a very sharp peak superposed in a broad overall distribution. The reason for this is that in the example taken, most of the four-lepton events are due to the decay of an A_H to W^+W^- followed by the leptonic decays of the W's. These events will not give rise to any invariant mass peak. But, there is a fraction of events where one A_H decays to a ZZ pair which then in turn can decay to four-leptons. This will give rise to a peak in M_{4l} as we see in Figure 3. Note that, the branching fraction of an A_H of mass 230 GeV to a pair of Z-bosons is around 22% while it is 77% to a pair of W's. Over and above that, the branching fraction of $W^\pm$ to charged leptons is greater than that of Z. This accounts for the spread of events away from the peak, as seen in Figure 3. One may also note that, in general, fewer 4-lepton events are expected in this model from leptonic cascades of the Z_H. This is because, for our choice of parameters, Z_H has the largest branching ratio in the hA_H channel.

Based on the above considerations, LHT-TPV and UED-KKV fall into category-1 while SUSY-RPV and UED-KKC belong to category-2. Note that, this classification for LHT-TPV is valid only for $A_H \geq 120$ GeV, so that it has sufficient branching fraction for $ZZ^{(*)}$. We shall discuss the other cases later in subsection 4.2.

Our task now is to distinguish between the look-alike models within each category. We do so in the following subsections.

4.2 Pairwise dilepton invariant mass distribution of the four leptons

One can go a little further in the task of model discrimination by combining the information from M_{4l} plots with distributions in the invariant mass distribution M_{ij} $(i, j = 1, 2)$ of the OS lepton pairs. Taking events with two pairs of opposite-sign leptons, we first order the leptons of each sign in the descending order of transverse momentum. In order to be sufficiently general in our analysis, no constraint on the flavour of the leptons is imposed while pairing them up. This is because, in SUSY-RPV, flavours of the leptons coming from neutralino decays are not correlated in general, apart from constraints coming from the antisymmetry in the first two indices of the λ_{ijk}-type terms in the superpotential. Thus in general we can form four possible pairs of opposite sign (OS) leptons.

For the models belonging to *category-2*, i.e., SUSY-RPV and UED-KKC, the M_{ij} distributions show no peaking behaviour. But, we see in the insets of Figure 4 that the M_{ij} distributions for UED-KKC show a prominent edge at $\sim$ 35 (50) GeV for point A (point B). We note that in 50% of the cases, the lepton pairs come from the same decay chain starting with a Z_1 (as described in detail in the context of angular correlation between the lepton-pairs in subsection 4.3). Therefore, an invariant mass edge is expected at the value given by $\sqrt{(M_{Z_1}^2 - M_{L_1}^2)(M_{L_1}^2 - M_{\gamma_1}^2)/M_{L_1}^2}$, which comes out to be 32.36 (50.95) GeV for

point A (point B).

For the SUSY-RPV point under consideration, we also see in Figures 4 and 5 an edge in the invariant mass distributions of two OS leptons near the corresponding neutralino mass. But as the two leptons in the pairs we consider have equal probability of coming from either the same chain or two different chains, the mass-edge in the distributions is smeared by the "wrong combinations". If one forms OS leptons pairs with a very small opening angle between them, the neutralino mass-edge will become very sharp. As the lightest neutralino mass can be as low as 46 GeV [16], the position of the invariant mass edge for UED-KKC and SUSY-RPV will not be very different for neutralino masses close to this bound. However, for neutralino masses higher than ~ 100 GeV, the edge positions will be quite different, as in UED-KKC the value obtained cannot be that large in any allowed region of the parameter space.

In case of models belonging to *category-1*, we can see from Figures 4 and 5 that the distributions for UED-KKV show a clear peak at the same value of M_{ij} for all the four possible cases. The peak is at the mass of γ_1 which is 475 (800) GeV for point A (point B). The two OS leptons coming from the decay of a γ_1 are expected to be of high transverse momentum, thereby constituting the majority of (11) pairs. Therefore, the peak height is very large for the M_{11} distribution. As we gradually consider OS combinations of softer leptons, the peak height reduces . This is because, most of the softer leptons come from intermediate stages of the cascade, and invariant mass distributions involving them will just give rise to a broad overall distribution. Therefore, in UED-KKV, as long as the LKP is the heavy photon, such an invariant mass peak is an unmistakable feature of the model. Here, one should also note that the position of the OS dilepton peak is always different from the position of the four-lepton peak as we obtain in UED-KKV. The difference, although not very large, can be observed at the LHC given the fact that the four-lepton channel is a rather clean one. Looking at Figures 3 and 4 we find that for point A, the M_{4l} peak is roughly at 509 GeV (M_{Z_1}) and the M_{ij} peaks are at 475 GeV (M_{γ_1}). Hence the difference between the values of these two peak positions, which in this case is around 34 GeV, is large enough to be measurable within the experimental resolutions at the LHC. Moreover, note that, these two peaks appear in two different distributions making the resolution even easier. Similar considerations apply for point B, too.

In the example considered here, the corresponding distributions for LHT-TPV also show a clear peak at the mass of the Z-boson (~ 90 GeV), as we can see from Figures 4 and 5. The Z-peak is superposed over a broad M_{ij} distribution coming from leptons from W's. Note that for point A, the branching fraction of $A_H \to ZZ$ is 22% and the corresponding branching fraction $A_H \to W^+W^-$ is 77%. Therefore, relatively fewer dilepton pairs come from the decay of a Z-boson and hence the fraction of events under the Z-peak is smaller compared to the total distribution. For point B, as the $A_H \to ZZ$ branching fraction increases to 35%, the peak at M_Z is even more prominent over the l^+l^- continuum coming from W^+W^-. This, however, is not generic to LHT-TPV. As discussed in detail in Ref. [56, 59], as far as the decays of A_H is concerned, there are essentially three possible cases for this model. For lower masses ($M_{A_H} \lesssim 120$ GeV, $f \lesssim 800$ GeV) the decay of A_H is dominated by the loop-induced two-body modes into fermions (case-1), whereas for higher masses ($M_{A_H} > 2M_W, f > 1070$ GeV) the two-body modes to gauge boson pairs dominate (case-3). For intermediate masses, both the two-body and three-body modes compete (in the three-body mode we have one off-shell

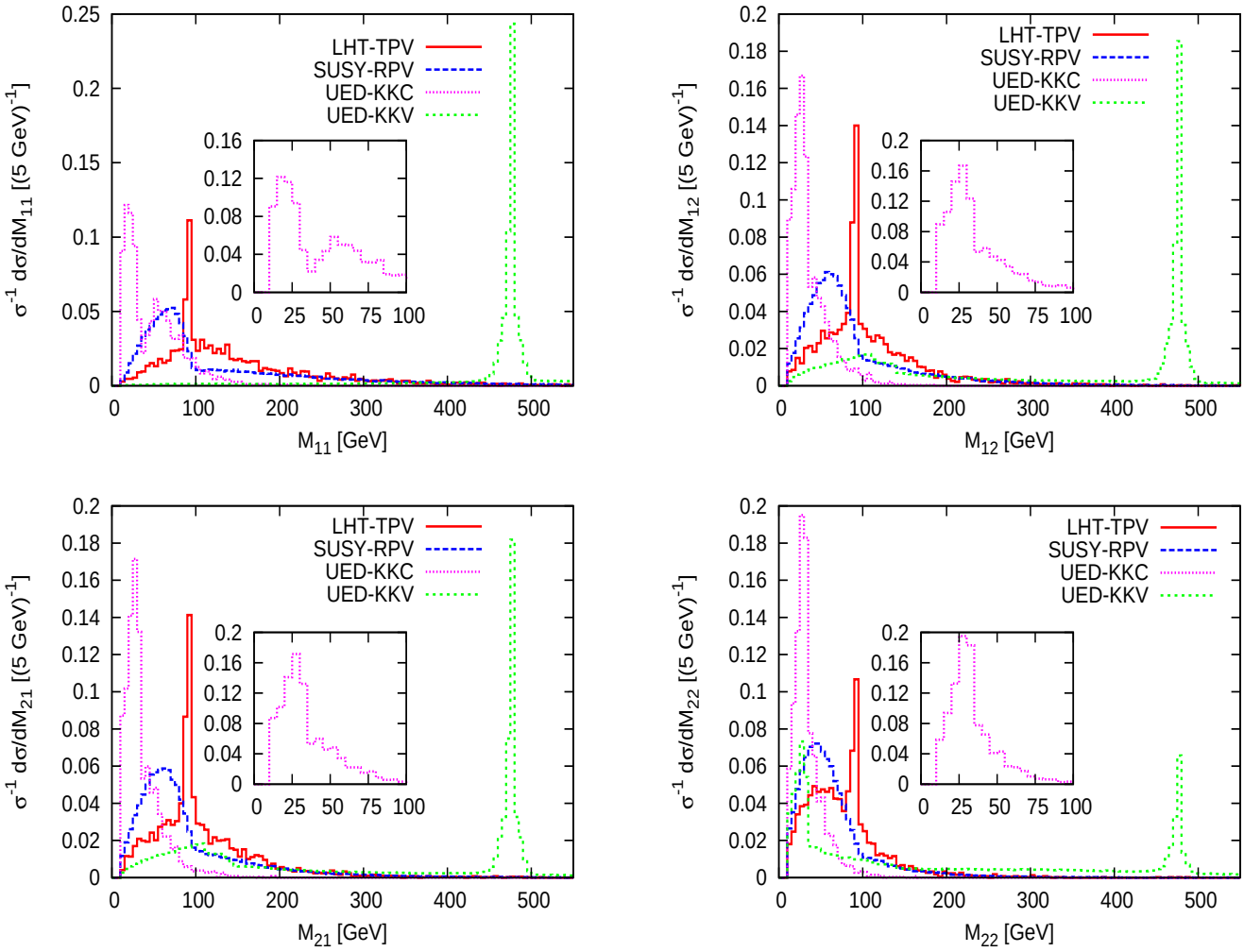

Figure 4: Normalized invariant mass distribution of OS lepton pairs formed out of the four leptons with total charge zero. The above distributions are for point A, at $\sqrt{s} = 14$ TeV, after Cut-2. The insets are shown in order to clearly identify the position of the invariant mass edge for UED-KKC.

$W^{\pm}$ or Z) (case-2). The points we have analysed here (point A and B), belong to case-3. For case-1 one would obtain a very clear peak in the OS dilepton invariant mass distribution but no peak in M_{4l}, while in case-2 a peak is expected in both OS dilepton and four-lepton distributions at the same mass-value. Therefore, case-1 will give rise to a situation where LHT-TPV belongs to category-2, but it will be distinguishable from SUSY-RPV and UED-KKC by its dilepton peak. And in case-2, LHT-TPV would belong to category-1, but it can still be distinguishable from UED-KKV by the fact that the OS dilepton and four-lepton peaks will be at the same mass-value for LHT-TPV, but at different values for UED-KKV. Moreover, in case -2, 120 GeV $\lesssim M_{A_H} \lesssim$ 160 GeV, and no peak is expected in UED-KKV at such a low value of the dilepton invariant mass. For details on the reconstruction of such

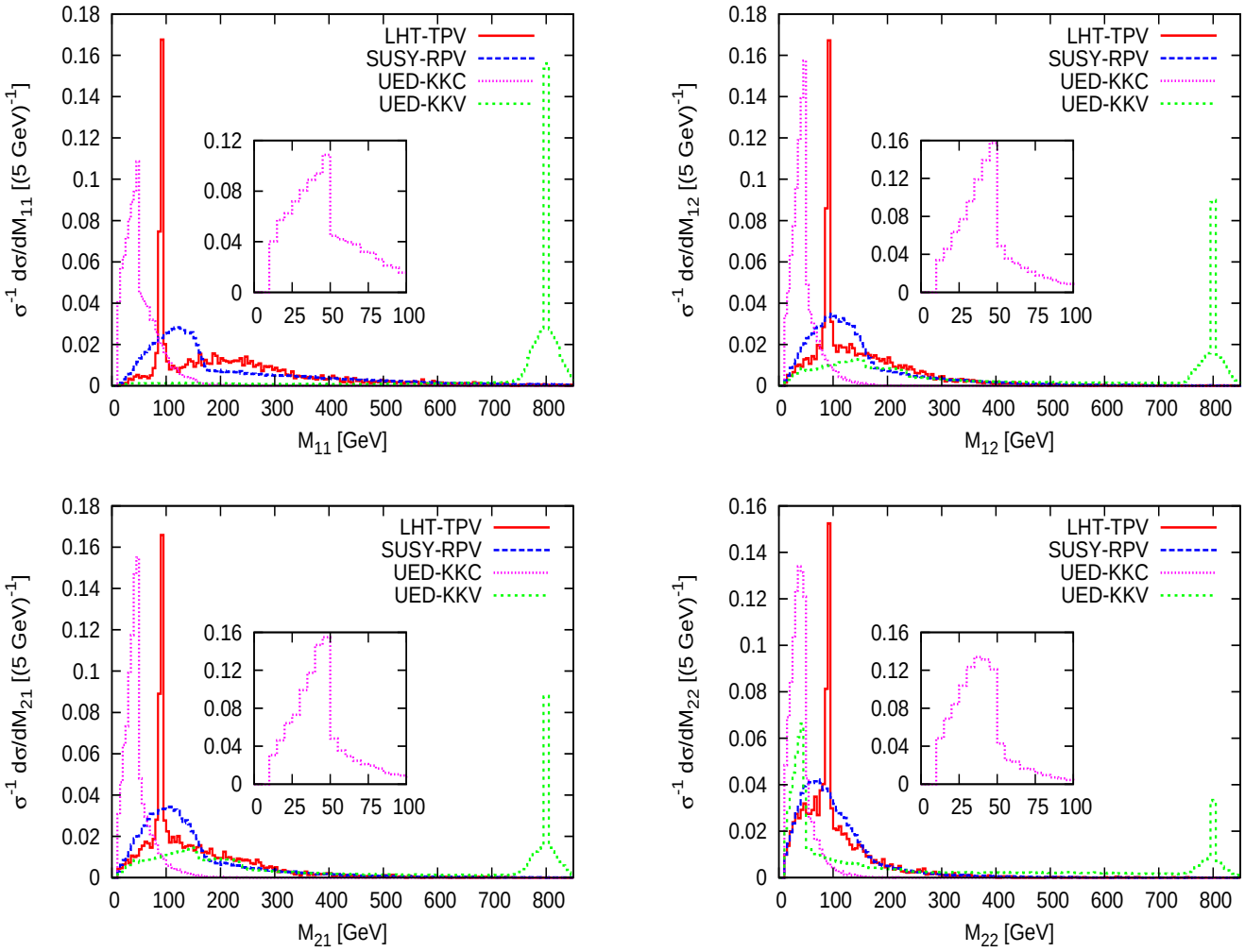

Figure 5: Same as Figure 4, for point B.

peaks above SM backgrounds in LHT-TPV, we refer the reader to Ref. [59]. Thus, we note that the features of OS dilepton invariant mass distributions, if used in conjunction with other important kinematic characteristics, can help in discriminating models belonging to different categories.

In addition to the invariant mass distributions of the different possible OS dilepton pairs formed out of the four leptons, it might also be useful to look into pairwise correlation of the different M_{ij}'s as shown in Figure 6. In this figure, for the purpose of illustration, we show the correlation of (M_{11}, M_{12}) and (M_{11}, M_{22}) for the various models at point A on an event-by-event basis (at $\sqrt{s} = 14$ TeV after Cut-2). We can see from Figure 6 that for the models where we observe peaks in the M_{ij} distributions, the (M_{11}, M_{12}) correlation plot shows two typical lines parallel to the M_{11} and M_{12} axes at the values of the peak-position (around 475 GeV for UED-KKV and 90 GeV for LHT-TPV). On the otherhand, for the models showing an edge in the M_{ij} distributions we see from the scatter plots that the

values of M_{ij} are mostly concentrated within the upper-bound given by the position of the edge (around 100 GeV for SUSY-RPV and 35 GeV for UED-KKC).

If both the OS dilepton pairs 11 and 22 come from a γ_1 in UED-KKV or a Z-boson in case of LHT-TPV, then M_{11} and M_{22} will have the same value (with an error-bar, due to detector effects etc.) in the corresponding event. That's why we expect a "blob" in the (M_{11}, M_{22}) plane as can be seen from Figure 6 for UED-KKV and LHT-TPV (centered around M_{γ_1} and M_Z respectively). For UED-KKC or SUSY-RPV, the boundedness of M_{ij}'s is once again reflected by the "box-like" distribution, the spread away from the boxes being significantly lesser than for the (M_{11}, M_{12}) case, as the leptons in the pair 22 are much softer. As we have four possible OS lepton pairings as explained before, one can have six different correlation plots between them. But all the essential features remain the same as in the two correlation plots we show for the various models.

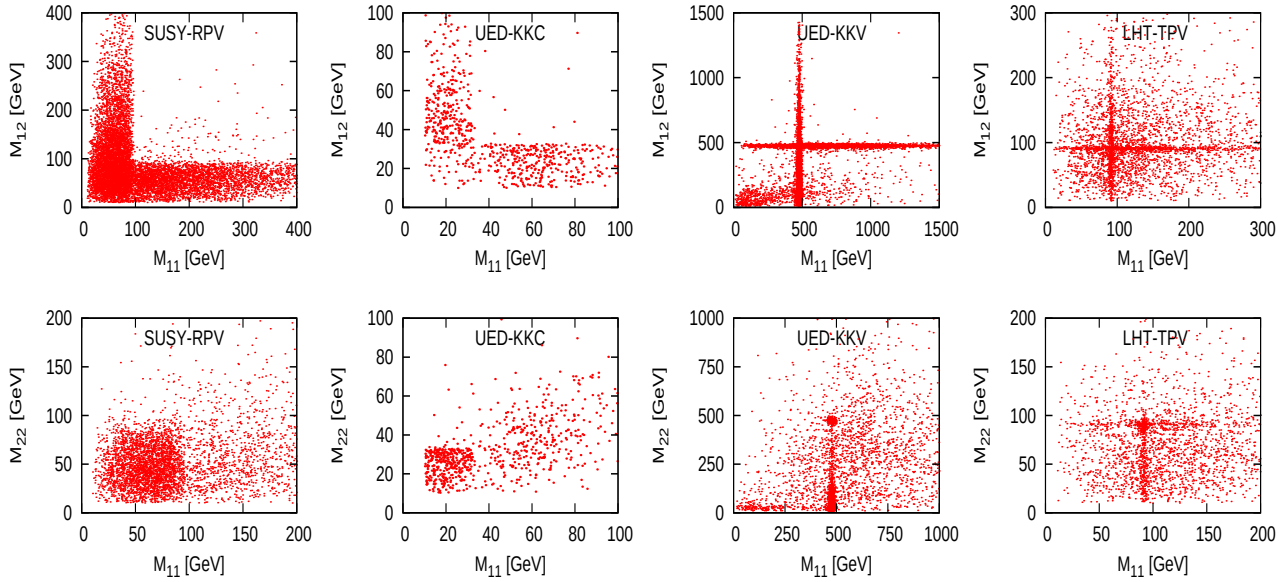

Figure 6: Pairwise correlation of opposite-sign dilepton invariant mass on an event-by-event basis for point A in various models at $\sqrt{s} = 14$ TeV, after Cut-2. We have shown two of the six possible correlations, the essential features in the rest being the same.

4.3 Pairwise angular correlation of the four leptons

In this subsection, we consider the correlation in the opening angle between the lepton pairs. The pairs have been formed out of the four leptons following the same prescription as used in the previous subsection.

In Figures 7 and 8 we have presented distributions of the cosine of the opening angle between the OS lepton pairs for point A and point B respectively. The opening angle is calculated in the lab frame and is defined by the relation

$$cos\theta_{ij} = \frac{\vec{p_i}.\vec{p_j}}{|\vec{p_i}||\vec{p_j}|} \; ; \quad i,j = 1,2 \tag{12}$$

where $\vec{p_i}$ and $\vec{p_j}$ stand for the momenta of positive and negatively charged leptons respectively.

In order to quantify the difference between the various models in the distribution of $cos\theta_{ij}$, we define the following asymmetry variable:

$$A_{ij} = \frac{\int_0^{+1} \frac{d\sigma}{dcos\theta_{ij}} d(cos\theta_{ij}) - \int_{-1}^{0} \frac{d\sigma}{dcos\theta_{ij}} d(cos\theta_{ij})}{\int_0^{+1} \frac{d\sigma}{dcos\theta_{ij}} d(cos\theta_{ij}) + \int_{-1}^{0} \frac{d\sigma}{dcos\theta_{ij}} d(cos\theta_{ij})}. \tag{13}$$

As we are considering the normalized distribution of $cos\theta_{ij}$ here, the denominator of A_{ij} as defined in Equation 13 will be 1. In Table 2 we show the values of A_{ij} in the different models under consideration.

Let us first consider the *models belonging to category-2*. We can see from Figures 7 and 8 that for SUSY-RPV, the distribution of $cos\theta_{ij}$ tends to peak towards +1.0. This is because the fraction of OS lepton pairs which are coming from the decay of a sufficiently boosted single neutralino tend to be highly collimated. The rest of the combinations (which include two leptons coming from two separate decay chains, or one coming from a chargino and another from a neutralino decay) will have OS leptons which are largely un-correlated. Thus we can see a overall flat distribution of $cos\theta_{ij}$ with a very significant peaking towards +1.0. For the same reason, the values of A_{ij} in SUSY-RPV in Table 2 are larger than in the other models for all i, j. We should note here that the boost of the neutralino is large, thanks to the substantial mass splitting among the gauginos usual in mSUGRA. In a generic MSSM model, the splittings might become smaller, thereby rendering the neutralinos less boosted and the distributions of $cos\theta_{ij}$ less sharply peaked towards +1.0.

For UED-KKC, we have two possibilities while forming the OS lepton pairs - the two leptons can either come from the same decay chain or they can come from two separate decay chains. In the former case, we expect the two OS leptons to have a smaller opening angle in general. This is because, they come from the decay chain $Z_1 \to l^+l^-\gamma_1$, where the parent Z_1 will be carrying the boost of the initially produced Q_1 . As the leptons themselves have very low p_T's in the rest frame of the Z_1, this boost of the Z_1 will make them collimated to an extent. For the second possibility, the leptons are, in many cases, nearly back-to-back as they come from the cascade decay of two Z_1's which for a significant fraction of events lie in two different hemispheres of the detector. For point A, the mass splittings are quite small between the $n = 1$ KK-excitations, whereas for point B, they are relatively larger. Since we have demanded two of the leptons to have p_T greater than 20 GeV, it is very likely from the point of view of UED mass splittings that for point A, in a larger fraction of events, both of the hard leptons will not come out from the same decay chain . Therefore, in a significant number of events, the combinations (12) and (21) are expected to be from the same chain, whereas the (11) and (22) pairs will involve both the decay chains. This leads us to expect the cosθ_{12} and cosθ_{21} distributions to be more peaked towards +1.0 than towards −1.0, while the cosθ_{11} and cosθ_{22} distributions have slight peaking near both +1.0 and −1.0. It can be readily verified that Figure 7 is in conformity with these observations. Similarly, we see from Table 2 that (for point A) the values of $A_{12}(= 0.34)$ and $A_{21}(= 0.34)$ are relatively higher and positive, implying significant asymmetry with more events having cos$\theta > 0$. We also note that $A_{11}(= 0.17)$ and $A_{22} = (0.12)$ indicate more symmetric distributions for cosθ_{11} and cosθ_{22} as discussed above. This asymmetry, however, is no longer expected if the mass-splittings become larger, as then the OS lepton pairs can come with equal probability from

both the chains. We observe this feature in case of point B in Figure 8 and also in Table 2. Therefore, in UED-KKC, the distribution of $\cos\theta_{ij}$ is in general *much less asymmetric towards* $+1.0$ as compared to SUSY-RPV.

Thus, based upon the above features, one should be able to distinguish between SUSY-RPV and UED-KKC. We shall see in what follows that there are also other features like the total charge of the four leptons, or the ratio of five or higher lepton to four-lepton cross-sections which can act as useful discriminators between the models belonging to category-2.

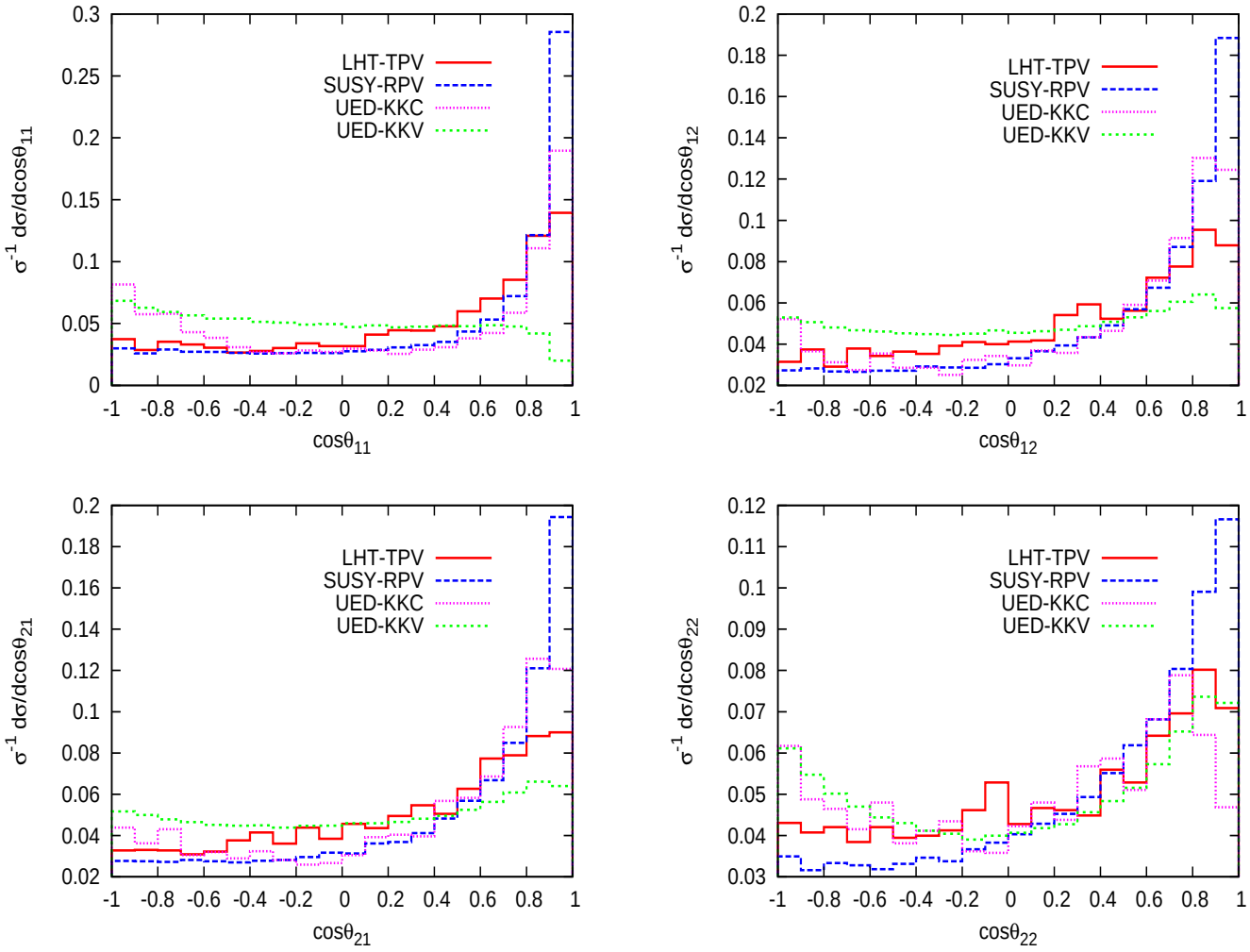

Figure 7: Normalized distribution of $\cos\theta_{ij}$ in the different models for point A at $\sqrt{s} =$ 14 TeV after Cut-2.

Next we consider the *models belonging to category-1*. In case of UED-KKV, the two OS leptons of highest p_T come in most cases from the decay of a γ_1 which itself has a very low p_T to start with. So, in the rest frame of γ_1, the two leptons will almost be back-to-back, leading to the slight peaking of $cos\theta_{11}$ towards -1.0 as seen from Figures 7 and 8. This interesting feature of UED-KKV is also reflected in the value of $A_{11} = -0.11$ (-0.24) for point A (point

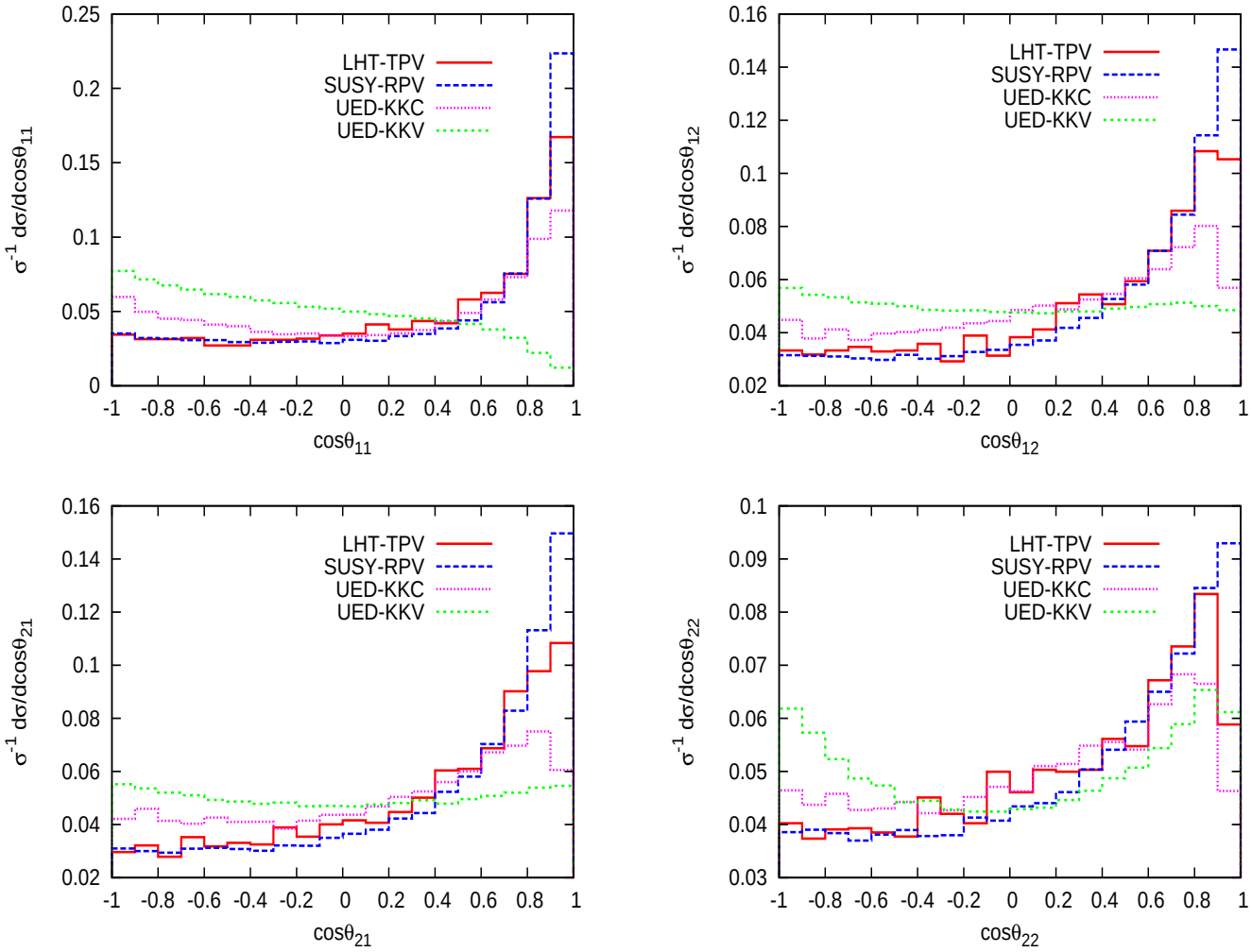

Figure 8: Normalized distribution of $\cos\theta_{ij}$ in the different models for point B at $\sqrt{s}$ = 14 TeV after Cut-2.

B). The distributions for $\cos\theta_{12}$ and $\cos\theta_{21}$ on the other hand are very flat indicating that these leptons have no angular correlation between them. This is not unexpected, since the combinations (12) and (21) will generally be formed when one of the leptons (the harder one with index 1) comes from the decay of γ_1, and the other, softer one, from the intermediate stages of the cascade (mostly from the decay of Z_1, W_1 or L_1). Therefore, A_{12} and A_{21} are close to zero as can be seen from Table 2. Finally, we see that the distribution for $\cos\theta_{22}$ shows a peaking behaviour towards both $+1.0$ and -1.0. This can be understood from the fact that the two softest leptons almost always come from the intermediate stages of the cascade where they emerge from either the decays of Z_1 and W_1. A large fraction of Z_1-initiated events gives rise to collimated leptons (giving rise to the peaking towards $+1.0$, while a significant fraction of events where the leptons come from W_1 will have them coming out in opposite directions (responsible for the peaking towards -1.0.

Finally, from all the distributions of cosθ_{ij} and the values of A_{ij} it is clear that the LHT-TPV model has features similar to SUSY-RPV. In particular, as the leptons come from the decays of a boosted A_H (via intermediate W^+W^- or ZZ states), they tend to be collimated. The collimation here is somewhat less than as in SUSY-RPV because of the fact that for the chosen parameters (point A), the squark (gluino)-neutralino mass difference ($\sim$ 471(509) GeV) is much larger than the q_H-A_H mass difference ($\sim$ 375 GeV).

Thus while both UED-KKV and LHT-TPV might give rise to clear peaks in the M_{4l} distribution, they show *entirely different behaviour* as far as the angular correlation between the OS lepton pairs is concerned. This, therefore, can act as a very good discriminator between these models belonging to category-1. In the following subsections, we shall look into some more variables that can be used to further clarify the distinction between these two models, especially when different types of mass-spectra in LHT-TPV tend to obliterate the $4l$ mass peaks so spectacular for our chosen benchmark points.

We should note here that there is a dip observable in the cosθ_{ij} distributions towards the last bin near +1.0 for UED-KKC and LHT-TPV. This dip, however, is not seen in the cosθ_{11} distribution. This is stemming from the fact that we have demanded all OS lepton pairs to have an invariant mass greater than 10 GeV. Now, when the lepton p_T's are not very high themselves, the invariant mass becomes very small when the angle between the leptons tends to zero. These events, therefore, have been removed by the above cut, giving rise to the observed dip. As for the (11) combination the leptons are much harder, the lepton pairs always pass the invariant mass cut, and this feature does not appear for this case.

Point A				
Variable	SUSY-RPV	LHT-TPV	UED-KKC	UED-KKV
A_{11}	0.46	0.37	0.17	-0.11
A_{12}	0.44	0.28	0.34	0.06
A_{21}	0.44	0.28	0.34	0.07
A_{22}	0.32	0.15	0.12	0.08
Point B				
A_{11}	0.39	0.38	0.16	-0.24
A_{12}	0.37	0.33	0.18	-0.02
A_{21}	0.38	0.33	0.16	5.27×10^{-4}
A_{22}	0.22	0.18	0.11	0.03

Table 2: Asymmetry variable (A_{ij}), as defined in eqn. 13, in the different models for point A and point B. The values quoted are at $\sqrt{s} = 14$ TeV, after Cut-2.

4.4 Total charge of the four-leptons

Here we consider the variable total charge (Q) of the four leptons obtained in the general channel $4l+ \geq 2j + \not{E}_T$. Q can take values in the set {-4,-2,0,2,4}. In Figures 9, 10 we see the distribution of Q for the different models. We observe that UED-KKC clearly stands out as in this case the four leptons come from two cascade decay chains starting with Z_1's

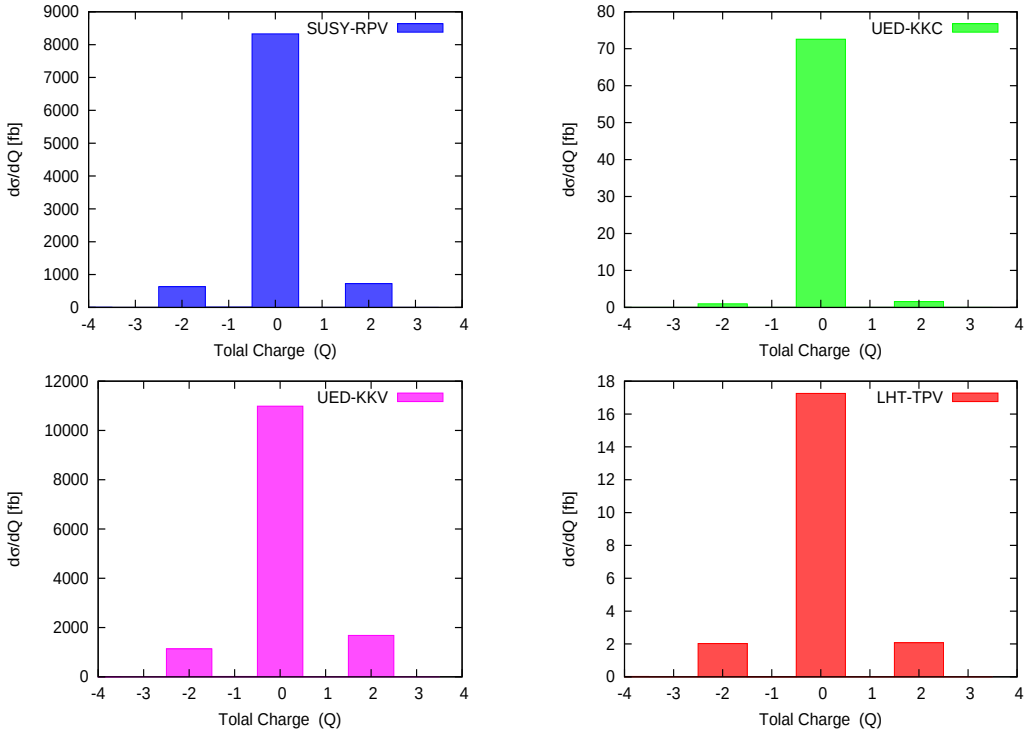

Figure 9: Total charge distribution of the four-leptons in the different models: for point A, at $\sqrt{s} = 14$ TeV, after Cut-2.

leading to $Q = 0$ for all the events. For the RPV coupling considered for point A, the lightest neutralino in SUSY-RPV always decays to a pair of leptons and a neutrino. If no other leptons come from the cascade, these four leptons will have a total charge $Q = 0$. On the other hand, if some additional leptons come from the decays of charginos or sleptons in the cascade, the lepton multiplicity in those events will be higher than four. It is however possible in a certain fraction of events to have a pair of leptons (coming from the decay of a single boosted neutralino) to be so highly collimated that they do not pass the lepton-lepton separation cut. These events might lead to a total charge $Q = \pm 2$. For LHT-TPV different combinations of W and Z decays can lead to four-lepton events. Hence, the expected values of Q are (-2,0,2). For UED-KKV, the leptons coming from the decay of γ_1 are always oppositely charged. But, it is possible to obtain W_1's of either charge from the cascades, giving rise to same-sign lepton pairs, over and above those coming from γ_1. This leads to $4l$ events with $Q = \pm 2$. Hence, essentially, from the distribution of Q, the UED-KKC model can be separated from the rest.

5 Five or higher lepton events

For all of the models discussed here, additional leptons, over and above those coming from sources discussed in the previous subsections, can come from various stages in the cascades.

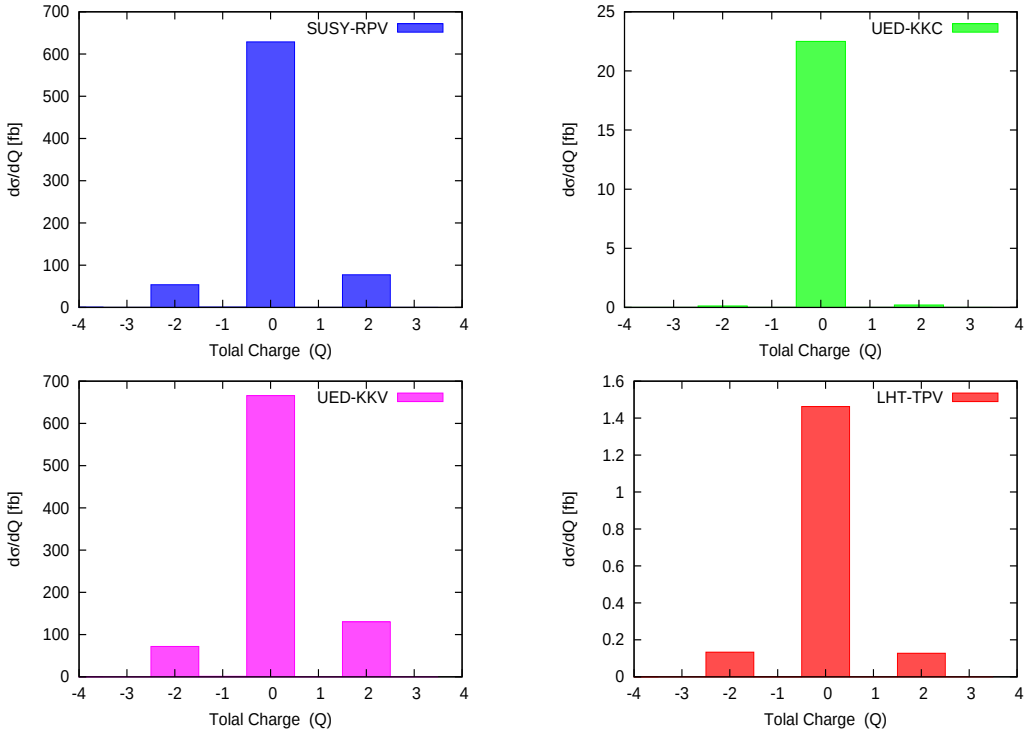

Figure 10: Same as Figure 9, for point B.

In Table 3, the rates for final states with five or more leptons are presented for our chosen benchmark points. The $p_T(E_T)$ cut has been uniformly maintained at 10 GeV for each lepton. The ratios of the five or higher lepton event rates to those for four-leptons are also presented. The SM backgrounds for channels with lepton multiplicity greater than four are negligible.

The rates for such added profusion of leptons depend on the respective spectra. The deciding factor here is the leptonic branching ratio for Z_2-odd particles at intermediate stages of the cascade. In this respect, UED-KKC and LHT-TPV fare worse. For UED-KKC, five-lepton events are not expected from the production and decays of the $n = 1$ KK-particles. Hence, the very small number of events with lepton multiplicity higher than four come from the decays of B-mesons, pions or photons. For LHT-TPV, with our choice of parameters, there are few additional leptons coming from the intermediate steps in the cascade. Therefore, in most of the $5l$ events found, the leptons are entirely coming from the decay of the two A_H's produced. One should note that this rate will increase for other choices of parameters, especially when the T-odd gauge bosons and the T-odd leptons are lighter than the T-odd quarks. For the SUSY-RPV examples considered, a proliferation of multilepton events is a well-known fact, and that is reflected in the high value of $\frac{\sigma(\geq 5l)}{\sigma(4l)}$. For point B, the ratio is higher (0.6) than for point A (0.35). This is because, as can be seen in section 2.2, in the former case, the SUSY mass spectrum is such that the chargino can decay to sleptons/sneutrinos, whereas in the later case such decays are not allowed by phase-space

Point A			
Model	$\sigma(4l)$ in fb	$\sigma(\geq 5l)$ in fb	$\frac{\sigma(\geq 5l)}{\sigma(4l)}$
SUSY-RPV	9450.91	3285.85	0.35
UED-KKC	163.36	1.57	0.01
UED-KKV	14008.93	4015.64	0.29
LHT-TPV	21.09	2.82	0.13
Point B			
SUSY-RPV	756.00	450.96	0.60
UED-KKC	26.24	0.12	0.005
UED-KKV	872.94	287.05	0.33
LHT-TPV	1.71	0.24	0.14

Table 3: Cross-section of four and five or more lepton events and the ratio $\frac{\sigma(\geq 5l)}{\sigma(4l)}$ for the different scenarios under consideration. The values tabulated are for point A and point B after isolation cuts and $p_T^l > 10$ GeV for all leptons, at $\sqrt{s} = 14$ TeV.

considerations. This leads to a higher branching fraction of obtaining a lepton from the cascade, thereby leading to relatively larger rates for events with higher lepton multiplicity in point B. For, UED-KKV, the ratio does not change significantly as we change the mass-scale. Therefore, we conclude that from this ratio, one can always single out the UED-KKC model. In the other models, there is enough room to change the ratios by adjusting the mass-spectra suitably.

6 Other possibilities

In addition to the kinds of new particle spectrum considered above, other possibilities of low missing energy look-alikes may offer themselves for detection as well as discrimination at the LHC. A few illustrative cases are discussed below.

In L-violating SUSY, we have a host of other possibilities. We considered the case of a neutralino LSP with a λ-type RPV coupling in our analysis. In the presence of λ'-type couplings instead, a neutralino will decay to two quarks and a charged lepton/ neutrino. Hence, the rate of four-lepton events will decrease. In addition, we shall not see the asymmetric peaking behaviour observed in the $cos\theta_{ij}$ distributions, too, since the lepton-pairs in this case will not be coming from the decay of a single boosted particle. Similarly, the edge in the dilepton invariant mass distributions will also not be present. There are, however, two features which distinguish this scenario from the rest. Firstly, the total charge distribution will now show a significant increase for $Q = \pm 4$. Secondly, with one lepton coming from each lightest neutralino during the SUSY cascades in two chains, a pair of same-sign dileptons occurs frequently at the end of the decay chains. Since the gluino, too, is of Majorana nature, being thereby able to produce charginos of either sign, there will be a surge in same-sign trilepton events observed [21].

A stau LSP scenario with λ-type couplings will also have similar implications. Here, stau

will decay to a lepton and a neutrino. If we have a stau LSP with λ'-type couplings instead, the 4l-signal will be suppressed, as the stau will decay to two quarks in this case. We also note that in presence of relatively larger values of λ'-type couplings, there is a region of the mSUGRA parameter space where the sneutrino can also become an LSP [6, 17]. However, the sneutrino in this case will decay to a pair of quarks thus reducing the possibility of having four leptons in the final state. Finally, we also remark that in the presence of bilinear R-parity violating terms, if we choose the RPV parameters to be consistent with the observed neutrino mass and mixing patterns, the neutralino LSP can decay to $W\mu$, $W\tau$ or $Z\nu$ [22]. Hence, four-lepton events will again be viable with a peak at M_Z in the OS dilepton invariant mass distributions. But there will not be any peak in the corresponding M_{4l} distribution. This last feature thus seems to be generically true in SUSY-RPV.

In the framework of a minimal UED model with KK-parity conservation, γ_1 is the LKP and characteristic signatures of this scenario were discussed throughout this article. The mUED model is based on the simplifying assumption that the boundary kinetic terms vanish at the cut-off scale Λ. This assumption restricts the mUED spectrum in such a way that the splittings among different KK excitations are small enough to result in soft final state particles and thus low missing E_T. As discussed in section A.2, the boundary terms receive divergent contributions and thus require counterterms. The finite parts of these counterterms remain undetermined and are therefore free parameters of the theory. This additional freedom could be exploited to end up with an unconstrained UED (UUED) scenario with several different possibilities:

- Particular combinations of the aforementioned free parameters can remove the degeneracy of the mUED mass spectrum. This results in harder leptons and jets in the final state and thus gives rise to a harder missing-E_T distribution. Such a version of the UED model no longer falls in the category of *low missing energy look-alikes*. The corresponding criteria for large missing-E_T scenarios will have to be applied in this situation [3].

- The values of the additional parameters could be chosen in such a way that even though the mass spectrum remains degenerate as in the case of mUED, the mass of ν_1 becomes smaller than M_{γ_1}. This leads to a scenario with ν_1 as the LKP and therefore, a possible candidate for cold dark matter. In this case, the γ_1's produced at the end of decay cascades will further decay into $\nu\nu_1$ pairs, resulting in similar phenomenology as in the case of mUED explored in this work. However, the four-lepton event rate in this case will be significantly reduced due to the fact that Z_1 mostly decays to $\nu\nu_1$ pairs, as this channel will now have enhanced phase-space available as compared to lL_1.

- One can also have such a combination of parameters that only the positions of Z_1 and $W_1^\pm$ in the $n = 1$ mass spectrum are altered. The first possibility is that Z_1 and $W_1^\pm$ are heavier than the $n = 1$ quarks. In such situations, $n = 1$ quarks will decay into qlL_1 via tree-level 3-body modes. L_1 subsequently decays into $l\gamma_1$ and combining the two cascade decay chains, one can then obtain four-lepton signals. However, the opposite-sign dilepton invariant mass distributions will not show any invariant mass edge in this scenario. The other possibility is that Z_1 and $W_1^\pm$ may become lighter than the $n = 1$ leptons. Here, the possible decay modes of interest are $Z_1 \to ll\gamma_1$

and $W_1^\pm \to l\nu\gamma_1$. Phenomenologically, this scenario will again be quite similar to the mUED cases we have studied.

In the framework of UED-KKV, the masses of the KK-fermions have a small dependence on the value of the KK-parity violating coupling h. As shown in Ref. [35], as we increase the value of h, the KK-fermion masses decrease. As the $n = 1$ quarks are much heavier than Z_1 and $W_1^\pm$ in mUED with KK-parity conserved, the presence of non-zero KK-violating coupling h does not lead to any appreciable change in the excited quark masses vis-a-vis those of the remaining particles. Therefore, the decay patterns of the $n = 1$ quarks remain the same. However, for smaller R^{-1}, singlet $n = 1$ leptons and the γ_1 are almost degenerate. Therefore, in addition to having a smaller R^{-1}, if we have a larger value of h, singlet $n = 1$ leptons may become lighter than γ_1. For example, this can happen for $R^{-1} = 500$ GeV and $h > 0.01$. Here, the only possible decay channel available for these singlet $n = 1$ leptons is via the KK-parity violating mode to a SM lepton of the same flavour and a Z/γ^*. The phenomenology of this scenario will be significantly different from the one we have considered so far with smaller values of h ($h \sim 0.001$) and a γ_1 LKP, and is therefore an interesting possibility for further studies.

In LHT-TPV, as we have two free parameters κ_q and κ_l which determine the masses of the T-odd quarks and leptons, the possibility of obtaining a fermionic LTP exists. In such cases, via the T-parity breaking terms, these fermions might decay to standard model particles. As observed in Ref. [56], there are two possible ways in which these fermionic LTP's can decay. As the WZW term breaks T-parity only in the gauge sector directly, a T-odd lightest fermion can decay by a three-body mode mediated by a virtual T-odd gauge boson. There is also the possibility of having loop-induced two-body decay modes. Therefore, the major decay channels are $f_H \to Zf$, $f_H \to W\tilde{f}$ and $f_H \to A_H^* f$. In the last case, the off-shell A_H might again decay to four-leptons via ZZ, but there will not be any peak in the M_{4l} distribution. On the other hand, if the LTP is a T-odd charged lepton, one can observe a spectacular five-lepton peak. The other possible decay modes will also lead to $4l$ and $5l$ events in varied rates, although the quantitative predictions of these will require us to determine the relative importance of the three-body and the loop-induced two body decay modes of f_H. A detailed phenomenology of this fermionic LTP scenario will be studied in a future work.

7 Summary and conclusions

We have considered four characteristic scenarios which can pass off as low missing energy look-alikes at the LHC. After convincing the reader that UED-KKC in its minimal form, in spite of containing a stable invisible particle, often falls in this category, we have studied the contribution of each scenario to events with four or more leptons. Since total rates alone, at the four-lepton level at least, can mislead one in the process of discrimination, we have resorted to kinematic features of final states in the different cases.

The first of these is the four-lepton invariant mass distribution. On this, we have found that the models get divided into two categories, depending on whether the four leptons show an invariant mass peak or not. While LHT-TPV and UED-KKV are in the first category, SUSY-RPV and and UED-KKC belong to the second one, thus offering a clear distinction.

For distinguishing between models within each category, we have used three observable quantities, namely, angular correlation and invariant mass of opposite-charge lepton pairs, and the total charge of the four observed leptons. It is found that angular correlations as well as the total charge causes SUSY-RPV to stand out quite clearly with respect to minimal UED-KKC. UED-KKV, too, stands out distinctly from the others, as far as angular correlations are concerned. This, however, still leaves room for discrimination. This happens, for example, where LHT-TPV has such a spectrum that the heavy photon LTP does not decay dominantly into four leptons. The distinction of this scenario with SUSY-RPV and UED-KKC is still possible using the pairwise invariant mass distribution of oppositely charged dileptons. We have also found that the relative positions of the dilepton vs. four-lepton invariant mass peaks, and the existence of an 'edge' in the dilepton invariant mass distribution lead to useful discriminating criteria. In addition, the ratio of five or higher lepton event rates to those for four leptons sets UED-KKC apart from the other scenarios.

As mentioned before, we haven't paid particular attention so far to the flavour content of the four leptons. In SUSY-RPV, depending upon the L-violating coupling chosen, the flavour content will change. However one can discover a pattern in the fraction of events with $4e$, 4μ, $2e2\mu$, $3e1\mu$ or $1e3\mu$, for specific RPV couplings (here e stands for the electron or positron and μ stands for the muon or anti-muon, and, for example, $3e1\mu$ means a four-lepton event with 3 e's and 1 μ). For the λ_{122} coupling that we chose for our analysis, we obtain, as expected, around 47.5% events to be of $1e3\mu$-type, whereas $2e2\mu$ and 4μ being $\sim 25\%$ each. No events are expected to be of $3e1\mu$ or $4e$-type. This is certainly a notable feature, but as observed above, these flavour ratios will change if we change the L-violating coupling. For UED-KKC one will always obtain $4e$, 4μ or $2e2\mu$-type events, while for UED-KKV all flavour combinations are possible. For LHT-TPV, depending upon the point of parameter space one is in, all flavour combinations are once again possible with varying fractions. Thus, although flavour content of the leptons can sometimes be useful, they might not be a very robust feature of the models, except for the case of UED-KKC.

We have also made a set of qualitative observations on other related scenarios such as RPV via λ'-type or bilinear terms, situations with stau or sneutrino LSP, UED-KKC with an unconstrained particle spectrum and different LTP (LKP) in LHT-TPV (UED-KKV). The qualitative changes that some of these scenarios entailed have been pointed out. On the whole, while the various theoretical models in their 'minimal' forms offer clear methods for distinction, a confusion can always be created in variants of the models with various degrees of complications. The same observation holds also for theories predicting large missing E_T. Thus one may perhaps conclude that, while some striking qualitative differences await one in the approach from 'data to minimal theories', there is no alternative to a threadbare analysis of the mass spectrum, possibly linking spin information alongside, if one really has to exhaust all possibilities that nature may have in store. Furthermore, the availability of data with high statistics, enabled by large accumulated luminosity, is of great importance. All this is likely to keep the highly challenging character of the LHC experiment alive till the last day of its run.

Appendix

A Description of the various models considered

A.1 SUSY with R-parity violation (SUSY-RPV)

The MSSM superpotential is given by [18]

$$W_{MSSM} = y^{l}{}_{ij} L_i H_1 \bar{E}_j + y^{d}{}_{ij} Q_i H_1 \bar{D}_j + y^{u}{}_{ij} Q_i H_2 \bar{U}_j + \mu H_1 H_2 \tag{A-1}$$

where H_1 and H_2 are the two Higgs superfields, L and Q are the SU(2)-doublet lepton and quark superfields and E, U, and D are the singlet lepton, up-type quark, and down-type quark superfields, respectively. μ is the Higgsino mass parameter and y_{ij}'s are the strengths of the Yukawa interactions.

If lepton and baryon number are allowed to be broken, the above superpotential can be augmented by the following terms [19]:

$$W_{\not R_p} = \lambda_{ijk} L_i L_j \bar{E}_k + \lambda'_{ijk} L_i Q_j \bar{D}_k + \lambda''{}_{ijk} \bar{U}_i \bar{D}_j \bar{D}_k + \epsilon_i L_i H_2. \tag{A-2}$$

where i, j, and k are flavour indices. Here the $\lambda''{}_{ijk}$ term leads to baryon number (B) violating interactions while the other three terms lead to the violation of lepton number (L). In MSSM, one imposes an additional discrete multiplicative symmetry known as R-parity which prevents any such term in the superpotential. R-parity is defined as $R_p = (-1)^{3B+L+2S}$, where S is the spin of the corresponding particle. This prevents, for example, terms which can lead to fast proton decay (although there are dangerous "R-even" dimension-five operators which can still lead to the decay of proton). However, the purpose is equally well-served if only *one* between B and L is conserved, R-parity violating (RPV) SUSY models are constructed with this in view. Of these, the versions containing L-violating interactions, trilinear and/or bilinear, have the added motivation of offering explanations of neutrino masses and mixing.

The consequences of RPV interactions have been explored extensively in the literature [19]. Especially, when L-violation takes place, although the conventional large missing E_T signature of SUSY is degraded, the possibility of obtaining multilepton final states is enhanced [20]. Recently, it has also been demonstrated that in presence of these L-violating operators, rather striking same-sign three-and four-lepton final states, which are free from SM backgrounds, are expected in large rates at the LHC [21].

In presence of the λ-type couplings, if the neutralino is the lightest supersymmetric particle (LSP), it will decay to a pair of leptons and a neutrino. Thus, starting from the pair production of squarks/gluinos in the initial parton level $2 \to 2$ hard scattering, we can obtain two neutralinos at the end of the decay cascade, which in turn can give rise to a four-lepton final state with unsuppressed rate for every SUSY process. Also, at least two additional jets will always be present from the decay of the squark pair. Thus, one can very easily obtain the $4l + nj + \not{E}_T$ ($n \geq 2$). If in addition to this, another lepton is produced from the cascade decay of a chargino, we can also obtain a five-lepton final state.

The λ'-type interactions, on the other hand, cause a neutralino LSP to decay into a lepton and two parton-level jets, this giving a dilepton final state for every SUSY particle production process. Four-lepton final states can arise through two additional leptons produced in

cascade, after the initial $2 \to 2$ process. Understandably, the probability of obtaining a four-lepton final state is suppressed compared to dilepton and trileptons.

The bilinear terms $\epsilon_i L_i H_2$ imply mixing between neutrinos and neutralinos as also between charged leptons and charginos [22]. Consequently, the lightest neutralino LSP can decay into a neutrino and the Z or a charged lepton and the W, the latter mode being of larger branching ratio. Thus, modulo the leptonic branching ratios of W-and Z-decay, one can have four-lepton final states, with an additional lepton in the cascade to account for the somewhat suppressed five-lepton final states in such a scenario.

It is clear from the above discussion that four-and five-lepton states are expected to have the highest rates in a situation with R-parity is broken through λ-type interactions alone, with two indices in λ_{ijk} being either 1 or 2. We, therefore, use this scenario as the benchmark for distinction from other theories through multilepton events. In situations including the other L-violating terms, the dilution in the branching ratio will affect the total rates of such final states (and, as we shall discuss later, the total rates are not very good guidelines in model distinction anyway). However, the kinematical observables on which our proposed distinction criteria are based are likely to remain mostly quite similar. We will comment on some special cases, including those where the lightest neutralino is not the LSP, in section 6.

A.2 Minimal universal extra dimension with KK-parity conservation (UED-KKC)

A rather exciting development in physics beyond the Standard Model (SM) in the last few years is the formulation of theories with compact spacelike extra dimensions whose phenomenology can be tested at the TeV scale. The idea is based on concepts first introduced by Kaluza and Klein [23] in the 1920's. Extra-dimensional theories can be divided into two main classes. The first includes those where the Standard Model (SM) fields are confined to a $(3 + 1)$ dimensional subspace (3-brane) of the full manifold. Models with the extra spacelike dimensions being both flat [24] or warped [25] fall in this category, although there have been numerous attempts to put some or all of the fields in the 'bulk' even within the ambits of these theories. On the other hand, there is a class of models known as Universal Extra Dimension(s) (UED) [26], where all of the SM fields can access the additional dimensions.

In the minimal version of UED (mUED), there is only one extra dimension y compactified on a circle of radius R (S_1 symmetry). The need to introduce chiral fermions in the resulting four-dimensional effective theory prompts one to impose additional conditions on the extra dimension. This condition is known as 'orbifolding' where two diametrically opposite ends of the compact dimension are connected by an axis about which there is a reflection symmetry.

The Z_2 symmetry breaks the translational invariance along the fifth dimension (denoted by the co-ordinate y) and generates two fixed points at $y = 0$ and $y = \pi R$. From a four-dimensional viewpoint, every field will then have an infinite tower of Kaluza-Klein (KK) modes, the zero modes being identified as the corresponding SM states. The spectrum is essentially governed by R^{-1} where R is the radius of the extra dimension.

UED scenarios can have a number of interesting phenomenological implications. These include a new mechanism of supersymmetry breaking [28], relaxation of the upper limit of the lightest supersymmetric neutral Higgs [29], addressing the issue of fermion mass hierarchy

from a different perspective [30] and lowering the unification scale down to a few TeVs [31, 32, 33].

In the absence of the orbifold fixed points, the component of momentum along the extra direction is conserved. From a four-dimensional perspective, this implies KK number conservation, where KK number is given by the position of an excited state in the tower. However, the presence of the two orbifold fixed points breaks the translational symmetry along the compact dimension, and KK number is consequently violated. In principle, one may have some additional interaction terms localised at these fixed points, causing mixing among different KK states. However, if these interactions are symmetric under the exchange of the fixed points (this is another Z_2 symmetry, not to be confused with the Z_2 of $y \leftrightarrow -y$), the conservation of KK number breaks down to the conservation of KK parity[1], given by $(-1)^n$, where n is the KK number. This not only implies that level-one KK-modes, the lightest among the new particles, are always produced in pairs, but also ensures that the KK modes do not affect electroweak processes at the tree level. The multiplicatively conserved nature of KK-parity implies that the lightest among the first excitations of the SM fields is stable, and a potential dark matter candidate [27].

The tree-level mass of a level-n KK particle is given by $m_n^2 = m_0^2 + n^2/R^2$, where m_0 is the mass associated with the corresponding SM field. Therefore, the tree level mUED spectrum is extremely degenerate and, to start with, the first excitation of any massless SM particle can be the lightest KK-odd particle (LKP). In practice, radiative corrections [34] play an important role in determining the actual spectrum. The correction term can be finite (bulk correction) or it may depend on Λ, the cut-off scale of the model (boundary correction). Bulk corrections arise due to the winding of the internal lines in a loop around the compactified direction [34], and are nonzero and finite only for the gauge boson KK-excitations. On the other hand, the boundary corrections are not finite, but are logarithmically divergent. They are just the counterterms of the total orbifold correction, with the finite parts being completely unknown. Assuming that the boundary kinetic terms vanish at the cutoff scale Λ the corrections from the boundary terms, for a renormalization scale μ, are proportional to $L_0 \equiv \ln(\Lambda^2/\mu^2)$. The bulk and boundary corrections for level-n doublet quarks and leptons (Q_n and L_n), singlet quarks and leptons (q_n and e_n) and KK gauge bosons (g_n, W_n, Z_n and B_n) are given by,

- Bulk corrections:

$$\begin{aligned} \delta\,(m_{B_n}^2) &= -\frac{39\,\zeta(3)\,a_1}{2\,\pi^2\,R^2}\ , \\ \delta\,(m_{W_n}^2) &= -\frac{5\,\zeta(3)\,a_2}{2\,\pi^2\,R^2}\ , \\ \delta\,(m_{g_n}^2) &= -\frac{3\,\zeta(3)\,a_3}{2\,\pi^2\,R^2}\ , \end{aligned} \tag{A-3}$$

  where, $\zeta(3) = \sum_{n=1}^{\infty} 1/n^3 \simeq 1.202$.

[1] In principle, it is possible to have fixed point localized operators that are asymmetric in nature [26]. This could violate KK-parity, analogous to the R-parity violation in supersymmetry. In absence of KK-parity the phenomenology of UED will be drastically different and will be discussed in brief in the next subsection.

- Boundary corrections:

$$
\begin{aligned}
\bar{\delta}\, m_{Q_n} &= m_n \left(3\, a_3 + \frac{27}{16}\, a_2 + \frac{a_1}{16}\right) L_0 \ , \quad \bar{\delta}\, m_{u_n} = m_n \,(3\, a_3 + a_1)\, L_0 \ , \\
\bar{\delta}\, m_{d_n} &= m_n \left(3\, a_3 + \frac{a_1}{4}\right) L_0 \ , \qquad \bar{\delta}\, m_{L_n} = m_n \left(\frac{27}{16}\, a_2 + \frac{9}{16}\, a_1\right) L_0 \ , \\
\bar{\delta}\, m_{e_n} &= \frac{9\, a_1}{4}\, m_n\, L_0 \ , \qquad \bar{\delta}\,(m^2_{B_n}) = -\frac{a_1}{6}\, m_n^2\, L_0 \\
\bar{\delta}\,(m^2_{W_n}) &= \frac{15\, a_2}{2}\, m_n^2\, L_0 \ , \qquad \bar{\delta}\,(m^2_{g_n}) = \frac{23\, a_3}{2}\, m_n^2\, L_0 \ , \\
\bar{\delta}\,(m^2_{H_n}) &= m_n^2 \left(\frac{3}{2}\, a_2 + \frac{3}{4}\, a_1 - \frac{\lambda_H}{16\pi^2}\right) L_0 + \overline{m}^2_H \ ,
\end{aligned}
\tag{A-4}
$$

where $a_i \equiv g_i^2/16\,\pi^2$, $i = 1 \ldots 3$, g_i being the respective gauge coupling constants and $\overline{m}^2_H$ is the boundary term for the Higgs scalar, which has been chosen to be zero in our study.

These radiative corrections partially remove the degeneracy in the spectrum [34] and, over most of the parameter space, γ_1, the first excitation of the hypercharge gauge boson (B), is the LKP [2]. The γ_1 can produce the right amount of relic density and turns out to be a good dark matter candidate [27]. The mass of γ_1 is approximately R^{-1} and hence the overclosure of the universe puts an upper bound on $R^{-1} < 1400$ GeV. The lower limit on R^{-1} comes from the low energy observables and direct search of new particles at the Tevatron. Constraints from $g-2$ of the muon [36], flavour changing neutral currents [37, 38, 39], $Z \to b\bar{b}$ [40], the ρ parameter [26, 41], other electroweak precision tests [42], etc. imply that $R^{-1} \gtrsim 300$ GeV. The masses of KK particles are also dependent on Λ, the cut-off of UED as an effective theory, which is essentially a free parameter. One loop corrected $SU(3)$, $SU(2)$ and $U(1)$ gauge couplings show power law running in the mUED model and almost meet at the scale $\Lambda = 20R^{-1}$ [31]. Thus one often takes $\Lambda = 20R^{-1}$ as the cut-off of the model. If one does not demand such unification, one can extend the value of Λ to about $40R^{-1}$, above which the $U(1)$ coupling becomes nonperturbative.

After incorporating the radiative effects, the typical UED spectrum shows that the coloured KK states are on top of the spectrum. Among them, g_1, the $n = 1$ gluon, is the heaviest. It can decay to both $n = 1$ singlet (q_1) and doublet (Q_1) quarks with almost the same branching ratio, although there is a slight kinematic preference for the singlet channel. q_1 can decay only to γ_1 and an SM quark. On the other hand, a doublet quark Q_1 decays mostly to W_1 or Z_1. Hadronic decay modes of W_1 and Z_1 are closed kinematically, so that they decay to different $n = 1$ doublet leptons. Similarly Z_1 can decay only to $L_1 l$ or $\nu_1 \nu$. The KK leptons finally decay to the γ_1 and SM leptons. Thus, the principal signals of such a scenario are n jets + m leptons + MET, where m can vary from 1 to 4.

A.3 mUED with KK-parity violation (UED-KKV)

Let us now briefly introduce KK-parity violation and its phenomenological consequences. As discussed in the previous subsection, operators localised at the orbifold fixed points

[2] The KK Weinberg angle is small so that $B_1 \approx \gamma_1$ and $W_1^3 \approx Z_1$.

give rise to mixing between different KK-states. In presence of such operators that are symmetric under exchange of the fixed points, even and odd KK-parity states mix separately, so that KK-parity is still a conserved quantity. However, it is possible to have fixed point operators which are asymmetric in nature, leading to the violation of KK-parity [26]. The phenomenology of KK-parity violation was studied in some detail in Ref. [35]. KK-parity violating couplings allow the LKP to decay into SM particles.

The asymmetry in the localised operators can be introduced by adding the following extra contribution to the operators localized at the point $y = 0$:

$$\mathcal{L}_f = \frac{\lambda}{\Lambda} \int \left[i\bar{\psi}\Gamma^\alpha D_\alpha \psi - i(D_\alpha \bar{\psi})\Gamma^\alpha \psi \right] \delta(y) dy, \tag{A-5}$$

where, $\psi(x^\mu, y)$ is the 5-dimensional fermion field, Γ^α are the gamma matrices and D_α are the covariant derivatives defined in (4+1) dimensions, λ is the strength of the KK-parity violating coupling, and Λ is the cut-off scale. The above operator has the following consequences:

- Equation A-5 gives rise to KK-parity violating mixing between KK-even and odd states. Of them, the mixing between $n = 0$ and $n = 1$ states are most relevant from the angle of the LHC phenomenology. The admixture of $n \geq 2$ KK-states with the $n = 0$ state is suppressed by the higher masses of the former.

- Equation A-5 leads to the coupling between two KK-fermions ($\psi^{(l)}$ and $\psi^{(m)}$) and a gauge boson ($A_\mu^{(n)}$): $ihg\bar{\psi}^{(l)}\gamma^\mu A_\mu^{(n)}\psi^{(m)}$, where h is a dimensionless coupling parametrised as $h = \lambda/(2\pi\Lambda R)$ and g is the gauge coupling. This coupling can be KK-parity violating, if $(-1)^{n+m+l} = -1$.

- In the KK-basis, interaction terms involving one $n = 0$ and two $n = 1$ particles are allowed by KK-parity. As an example consider the terms $ig\bar{\psi}_{KK}^{(1)}\gamma^\mu A_\mu^{(1)}\psi_{KK}^{(0)}$, $ig\bar{\psi}_{KK}^{(1)}\gamma^\mu A_\mu^{(0)}\psi_{KK}^{(1)}$ etc., where $\psi_{KK}^{(n)}$ is level-n fermion in the KK-basis. As a result of the mixing between $n = 0$ and 1 fermions , the above interactions give rise to KK-parity violating couplings between two $n = 0$ particles with one $n = 1$ particle in the mass eigenstate basis.

We have only considered the consequences of the fermionic kinetic terms localized at the point $y = 0$. However, in principle, one could also introduce kinetic terms for the 5-dimensional gauge bosons at $y = 0$. Such terms would lead to KK-parity violating decay of $n = 1$ gauge bosons into a pair of SM electroweak gauge bosons. For $W_1^\pm$ and Z_1-boson, the KK-parity conserving decays are overwhelmingly dominant. Therefore, the KK-parity violating decays of $W_1^\pm$ and Z_1-boson are phenomenologically insignificant. On the other hand, the LKP (γ_1), being completely B_1 dominated, can not have any coupling with the SM ZZ or W^+W^- pairs. Therefore, from the point of view of collider phenomenology, the KK-parity violating kinetic terms for the 5-dimensional gauge bosons are not significant.

We have already noted that, as a consequence of KK-parity violation, the lightest $n = 1$ particle decays into two or more SM particles. Thus, γ_1 can decay into SM fermion-antifermion pairs. The KK-parity violating couplings of γ_1 with the SM fermions are given by

$$\mathcal{L}_{KKV} = \frac{eh}{\sqrt{2}\cos\theta_W} \bar{f}[Y_L\gamma_\mu(1-\gamma_5) - Y_R\gamma_\mu(1+\gamma_5)]\gamma_1^\mu f, \tag{A-6}$$

where f is a SM fermion and Y_L and Y_R are the hypercharges of f_L andf_R respectively. For $\lambda \sim 1$ and $\Lambda R \sim 20$, the maximum value of the parameter h is $h_{max} \sim 0.01$. In our analysis, we take h to be same for all fermionic flavours. With this assumption, the decay branching fraction of γ_1 becomes independent of the value of h. We obtain 53.3% branching fraction for $\gamma_1 \to q\bar{q}$ and 38.9 (7.8)% branching fraction for $\gamma_1 \to l\bar{l}$ ($\nu\bar{\nu}$). For small values of the parameter h, the decay branching fractions of other $n = 1$ particles are insensitive to KK-parity violation, since such effects are suppressed by the cut-off scale Λ, so that they cannot compete with the KK-parity conserving modes. Therefore, the only phenomenological difference between UED-KKC and UED-KKV is the decay of the LKP and its decay gives rise to additional jets and leptons in the final states of UED cascades. Thus the additional leptons lead to rather clean signatures with the possibility of reconstructing the γ_1 as an invariant mass peak. On the whole, depending on whether either or both of the pair-produced γ_1's decay leptonically, the lepton multiplicity of the ensuing final states may vary between 0 and 8.

A.4 Littlest Higgs model with T-parity violation (LHT-TPV)

Little Higgs models [43, 44] have been proposed a few years ago to explain electroweak symmetry breaking and, in particular, to solve the so-called little hierarchy problem [45]. Among the different versions of this approach, the littlest Higgs model [46] achieves the cancellation of quadratic divergences with a minimal number of new degrees of freedom. In the LHT, a global $SU(5)$ symmetry is spontaneously broken down to $SO(5)$ at a scale $f \sim 1$ TeV. An $[SU(2) \times U(1)]^2$ gauge symmetry is imposed, which is simultaneously broken to the diagonal subgroup $SU(2)_L \times U(1)_Y$, the latter being identified with the SM gauge group. This leads to four heavy gauge bosons $W_H^{\pm}, Z_H$ and A_H with masses $\sim f$ in addition to the SM gauge fields. The SM Higgs doublet is part of an assortment of pseudo-Goldstone bosons which result from breakdown of the global symmetry. This symmetry protects the Higgs mass from quadratically divergent corrections. The multiplet of Goldstone bosons contains a heavy $SU(2)$ triplet scalar Φ as well. In contrast to SUSY, the new states which cancel the quadratically divergent contributions to the Higgs mass due to the top quark, gauge boson and Higgs boson loops, respectively, are heavy fermions, additional gauge bosons and triplet Higgs states.

In order to comply with strong constraints from electroweak precision data on the Littlest Higgs model [47], and at the same time ensure that the scale of new physics be not so high as to cause the so-called little hierarchy problem, one further imposes a discrete symmetry called T-parity [48]. It maps the two pairs of gauge groups $SU(2)_i \times U(1)_i, i = 1, 2$ into each other, forcing the corresponding gauge couplings to be equal, with $g_1 = g_2$ and $g_1' = g_2'$. All SM particles, including the Higgs doublet, are even under T-parity, whereas the four additional heavy gauge bosons and the Higgs triplet are T-odd. The top quark has two heavy fermionic partners, T_+ (T-even) and T_- (T-odd). For consistency of the model, one has to introduce the additional heavy, T-odd vector-like fermions u_H^i, d_H^i, e_H^i and ν_H^i $(i = 1, 2, 3)$ for each SM quark and lepton field. For further details on the LHT, we refer the reader to references [49, 50, 51, 52, 53].

The masses of the heavy gauge bosons in the LHT are given by

$$M_{W_H} = M_{Z_H} = gf\left(1 - \frac{v^2}{8f^2}\right) \approx 0.65f, \qquad M_{A_H} = \frac{fg'}{\sqrt{5}}\left(1 - \frac{5v^2}{8f^2}\right) \approx 0.16f, \tag{A-7}$$

where corrections $\mathcal{O}(v^2/f^2)$ are neglected in the approximate numerical values. Thus these particles have masses of several hundreds of GeV for $f \sim 1$ TeV, although A_H, the heavy partner of the photon, can be quite light, because of the small prefactor, and is usually assumed to be the LTP. When T-parity is unbroken, the LTP is stable, and gives rise to large MET signatures together with energetic jets and leptons from the cascades of heavy T-odd particles at the LHC. The masses of the heavy, T-odd fermions are determined by general 3×3 mass matrices in the (mirror) flavor space, $m^{ij}_{q_H,l_H} \sim \kappa^{ij}_{q,l} f$ with $i, j = 1, 2, 3$. We simplify our analysis by assuming that $\kappa^{ij}_q = \kappa_q \delta^{ij}$. The parameter $\kappa_q \sim \mathcal{O}(1)$ thus determines the masses of the heavy quarks in the following way:

$$m_{u_H} = \sqrt{2}\kappa_q f\left(1 - \frac{v^2}{8f^2}\right), \qquad m_{d_H} = \sqrt{2}\kappa_q f, \tag{A-8}$$

thereby allowing the new heavy quarks to have masses ranging from several hundreds of GeV to a TeV, for $f \sim 1$ TeV. Similarly, the masses of the heavy leptons in the spectrum are determined by a common parameter κ_l. For our study we have kept $\kappa_l = 1$. Note that these heavy quarks and leptons cannot be decoupled from the model as there is an upper bound $\kappa \leq 4.8$ (for $f = 1$ TeV) obtained from 4-fermion operators [53].

The A_H, however, can decay if T-parity is violated. This can happen via the so-called Wess-Zumino-Witten (WZW) term [54], which, according to Ref. [55], can be written as follows:

$$\Gamma_{\rm WZW} = \frac{N}{48\pi^2}\left(\Gamma_0[\Sigma] + \Gamma[\Sigma, A_l, A_r]\right). \tag{A-9}$$

The functional $\Gamma_0[\Sigma]$ is the ungauged WZW term which depends only on the non-linear sigma model field Σ. The term $\Gamma[\Sigma, A_l, A_r]$ is the gauged part of the WZW term.The explicit expressions for the functionals and the relation of the fields $A_{l,r}$ to the gauge fields in the LHT can be found in Ref. [55]. While these functionals are uniquely given by the symmetry breaking pattern $SU(5) \to SO(5)$ and the gauged subgroups in the LHT, the integer N in Eq. (A-9) depends on the ultraviolet (UV) completion of the LHT. In strongly coupled underlying theories it will be related to the representation of the fermions whose condensate acts as order parameter of the spontaneous symmetry breaking. In the simplest case, N will simply be the number of 'colors' in that UV completion, as is the case for the WZW term in ordinary QCD. The overall coefficient $N/48\pi^2$ encapsulates the effect of the chiral anomaly, which is a one-loop effect in the corresponding high-scale theory.

As noted in Ref. [55], the WZW term in Eq. (A-9) is not manifestly gauge invariant. Gauge invariance is violated by terms with an odd number of T-odd gauge bosons, such as one of the form $\epsilon_{\mu\nu\rho\sigma} V^\mu_H V^\nu \partial^\rho V^\sigma$, where V_H is a T-odd gauge boson and V denotes a SM gauge boson. Such anomalous terms need to be cancelled [55]. After the cancellation, the leading T-odd interactions appear only at order $1/f^2$. For instance, we get a vertex with one T-odd gauge boson and two SM gauge bosons from $\epsilon_{\mu\nu\rho\sigma}(H^\dagger H/f^2) V^\mu_H V^\nu \partial^\rho V^\sigma$, after the Higgs doublet H gets a vacuum expectation value v.

To leading order in $1/f$, the part of the WZW term containing one neutral T-odd gauge boson is given, in unitary gauge, by

$$\begin{aligned}\Gamma_n = \frac{Ng^2g'}{48\pi^2 f^2}\int d^4x\,(v+h)^2\,\epsilon_{\mu\nu\rho\sigma}\times \\ \left[-(6/5)A_H^\mu\left(c_w^{-2}Z^\nu\partial^\rho Z^\sigma + W^{+\nu}D_A^\rho W^{-\sigma} + W^{-\nu}D_A^\rho W^{+\sigma} + i(3gx_w + g's_w)W^{+\nu}W^{-\rho}Z^\sigma\right)\right. \\ \left.+t_w^{-1}Z_H^\mu\left(2c_w^{-2}Z^\nu\partial^\rho Z^\sigma + W^{+\nu}D_A^\rho W^{-\sigma} + W^{-\nu}D_A^\rho W^{+\sigma} - 2i(2gc_w + g's_w)W^{+\nu}W^{-\rho}Z^\sigma\right)\right].\end{aligned} \tag{A-10}$$

Here h is the physical Higgs boson, $D_A^\mu W^{\pm\nu} = (\partial^\mu \mp ieA^\mu)W^{\pm\nu}$ and s_w, c_w and t_w denote the sine, cosine and tangent of the weak mixing angle, respectively. All T-violating vertices with up to four legs have been tabulated in Ref. [56] and implemented into a model file for CalcHEP 2.5 [8, 57].

If A_H is heavy, the vertices in Eq. (A-10) lead to its decay into a pair of Z-bosons or into W^+W^- with a decay width of the order of eV [58]. On the other hand, if $M_{A_H} < 2M_W$, the heavy photon cannot decay into on-shell SM gauge bosons. It could still decay into (one or two) off-shell SM gauge bosons, but for low masses loop-induced decays into SM fermions will dominate. In fact, as discussed in Ref. [56], the T-violating vertices can couple the A_H to two SM fermions via a triangle loop. But since the corresponding one-loop diagrams are logarithmically divergent, one needs to add counterterms to the effective Lagrangian of the form

$$\mathcal{L}_{\rm ct} = \bar{f}\gamma_\mu\left(c_L^f P_L + c_R^f P_R\right) f A_H^\mu, \tag{A-11}$$

$$c_i^f = c_{i,\epsilon}^f\left(\frac{1}{\epsilon} + \log(\mu^2) + \mathcal{O}(1)\right), \tag{A-12}$$

where $P_{L,R} = (\mathbf{1} \mp \gamma_5)/2$.

The coefficients $c_i^f(\mu)$ of the counterterms can be estimated by naive dimensional analysis or naturalness arguments. The coefficients $c_{i,\epsilon}^f$ are explicitly listed in Ref. [56] and we have included the vertices from Eq. (A-11) in the CalcHEP model file.

The prefactor of the WZW term, $N/48\pi^2$, is of the size of a one-loop effect, thus the coupling of A_H and other T-odd gauge bosons to SM fermions via a triangle-loop is effectively 2-loop suppressed. Therefore these T-violating couplings will not affect the production mechanism of T-odd particles and their cascade decays at colliders, or EW precision observables [56]. In particular, T-parity violation should still satisfy the EW data with a rather small scale f. It is only in decays of the A_H that the anomaly term acquires phenomenological importance.

Let us briefly note here how four or higher lepton events can arise in LHT-TPV. All cascades initiated though the production of T-odd particles (notably the heavy T-odd quarks that are produced via strong interaction) lead to a pair of A_H. If kinematically allowed, the principal decay modes of the A_H are $A_H \to WW^{(*)}$ or $A_H \to ZZ^{(*)}$. Thus, four leptons can come from the leptonic decays of two Z-bosons, four W's, or two W's and one Z-boson (every event will have two A_H's produced at the end the cascades). We shall also discuss about the other possibilities section 4.2, where the loop-induced decay of each A_H to lepton pairs might also lead to four-lepton events [56, 59]. One can also have additional leptons from the

cascades if the initially produced heavy quarks can cascade decay to T-odd gauge bosons ($W_H^{\pm}$, Z_H) or T-odd leptons ($l_H^{\pm}$, ν_H). The two A_H's can further give rise to five lepton events if one of them decays to four-leptons (via ZZ) and the other decays to W^+W^-, one of which then decays semi-leptonically.

Acknowledgments

This work was partially supported by funding available from the Department of Atomic Energy, Government of India, for the Regional Centre for Accelerator-based Particle Physics (RECAPP), Harish-Chandra Research Institute. SM and BM acknowledge the hospitality of the Department of Theoretical Physics, Indian Association for the Cultivation of Science, Kolkata.

References

[1] N. Arkani-Hamed, G. L. Kane, J. Thaler and L. T. Wang, JHEP **0608** (2006) 070.

[2] J. Hubisz, J. Lykken, M. Pierini and M. Spiropulu, Phys. Rev. D **78**, 075008 (2008).

[3] A. Datta, G. L. Kane and M. Toharia, arXiv:hep-ph/0510204.

[4] P. Meade and M. Reece, Phys. Rev. D **74**, 015010 (2006); L. T. Wang and I. Yavin, JHEP **0704**, 032 (2007); M. M. Nojiri and M. Takeuchi, Phys. Rev. D **76**, 015009 (2007); C. Kilic, L. T. Wang and I. Yavin, JHEP **0705**, 052 (2007); A. Datta *et al.*, Phys. Lett. B **659**, 308 (2008); G. Hallenbeck *et al.*, Phys. Rev. D **79** (2009) 075024; A. Belyaev *et al.*, Pramana **72**, 229 (2009); B. Bhattacherjee *et al.*, Phys. Rev. D **81** (2010) 035021.

[5] T. Sjöstrand *et al.*, JHEP **0605**, 026 (2006).

[6] B. C. Allanach *et al.*, Phys. Rev. D **75**, 035002 (2007).

[7] A. Djouadi *et al.*, Comput. Phys. Commun. **176**, 426 (2007).

[8] A. Pukhov, arXiv:hep-ph/0412191.

[9] A. Datta, K. Kong and K. T. Matchev, arXiv:1002.4624 [hep-ph].

[10] J. Alwall *et al.*, arXiv:0712.3311 [hep-ph]; P. Skands *et al.*, JHEP **0407**, 036 (2004).

[11] M. L. Mangano *et al.*, JHEP **0307**, 001 (2003).

[12] J. Pumplin *et al.*, JHEP **0207**, 012 (2002).

[13] M. R. Whalley, D. Bourilkov and R. C. Group, arXiv:hep-ph/0508110.
`http://projects.hepforge.org/lhapdf/`

[14] G. Aad *et al.* [The ATLAS Collaboration], arXiv:0901.0512 [hep-ex]; G. L. Bayatian *et al.* [CMS Collaboration], J. Phys. G **34**, 995 (2007).

[15] Bruce Mellado, private communication.

[16] C. Amsler *et al.* [Particle Data Group Collaboration], Phys. Lett. **B667**, 1 (2008).

[17] M. A. Bernhardt *et al.* Phys. Rev. D **79** (2009) 035003.

[18] S. P. Martin, "A supersymmetry primer," arXiv:hep-ph/9709356, and references therein.

[19] For a review see, for example, R. Barbier *et al.*, Phys. Rept. **420**, 1 (2005).

[20] H. Baer, C. Kao and X. Tata, Phys. Rev. D **51** (1995) 2180.

[21] B. Mukhopadhyaya and S. Mukhopadhyay, arXiv:1005.3051 [hep-ph].

[22] S. Roy and B. Mukhopadhyaya, Phys. Rev. D **55**, 7020 (1997); B. Mukhopadhyaya, S. Roy and F. Vissani, Phys. Lett. B **443**, 191 (1998); M. Hirsch *et al.*, Phys. Rev. D **62**, 113008 (2000).

[23] T. Kaluza, Sitzungsber. Preuss. Akad. Wiss. Berlin (Math. Phys.) **1921**, 966 (1921); O. Klein, Z. Phys. **37**, 895 (1926).

[24] I. Antoniadis, Phys. Lett. B **246**, 377 (1990); N. Arkani-Hamed, S. Dimopoulous and G. Dvali, Phys. Lett. B **429**, 263 (1998); I. Antoniadis, N. Arkani-Hamed, S. Dimopoulos and G. R. Dvali, Phys. Lett. B **436**, 257 (1998).

[25] L. Randall and R. Sundrum, Phys. Rev. Lett. **83**, 3370 (1999); *ibid* **83**, 4690 (1999).

[26] T. Appelquist, H. C. Cheng and B. A. Dobrescu, Phys. Rev. D **64** (2001) 035002; H. C. Cheng, K. T. Matchev and M. Schmaltz, Phys. Rev. D **66** (2002) 056006.

[27] G. Servant and T. M. P. Tait, Nucl. Phys. B **650** (2003) 391.

[28] I. Antoniadis, Phys. Lett. B **246** (1990) 377.

[29] G. Bhattacharyya, S. K. Majee and A. Raychaudhuri, Nucl. Phys. B **793** (2008) 114.

[30] N. Arkani-Hamed and M. Schmaltz, Phys. Rev. D **61** (2000) 033005.

[31] K. Dienes, E. Dudas, and T. Gherghetta; Nucl. Phys. B **537** (1999) 47.

[32] K. R. Dienes, E. Dudas and T. Gherghetta, Phys. Lett. B **436** (1998) 55; For a parallel analysis based on a minimal length scenario, see S. Hossenfelder, Phys. Rev. D **70** (2004) 105003.

[33] G. Bhattacharyya, A. Datta, S. K. Majee and A. Raychaudhuri, Nucl. Phys. B **760** (2007) 117.

[34] H. C. Cheng, K. T. Matchev and M. Schmaltz, Phys. Rev. D **66**, 036005 (2002).

[35] B. Bhattacherjee, Phys. Rev. D **79** (2009) 016006.

[36] P. Nath and M. Yamaguchi, Phys. Rev. D **60** (1999) 116006.

[37] D. Chakraverty, K. Huitu and A. Kundu, Phys. Lett. B **558** (2003) 173.

[38] A.J. Buras, M. Spranger and A. Weiler, Nucl. Phys. B **660** (2003) 225; A.J. Buras, A. Poschenrieder, M. Spranger and A. Weiler, Nucl. Phys. B **678** (2004) 455.

[39] K. Agashe, N.G. Deshpande and G.H. Wu, Phys. Lett. B **514** (2001) 309.

[40] J.F. Oliver, J. Papavassiliou and A. Santamaria, Phys. Rev. D **67** (2003) 056002.

[41] T. Appelquist and H. U. Yee, Phys. Rev. D **67** (2003) 055002.

[42] T.G. Rizzo and J.D. Wells, Phys. Rev. D **61** (2000) 016007; A. Strumia, Phys. Lett. B **466** (1999) 107; C.D. Carone, Phys. Rev. D **61** (2000) 015008.

[43] N. Arkani-Hamed, A. G. Cohen and H. Georgi, Phys. Lett. B **513**, 232 (2001); N. Arkani-Hamed, A. G. Cohen, T. Gregoire and J. G. Wacker, JHEP **0208**, 020 (2002).

[44] For reviews, see M. Schmaltz and D. Tucker-Smith, Ann. Rev. Nucl. Part. Sci. **55**, 229 (2005); M. Perelstein, Prog. Part. Nucl. Phys. **58**, 247 (2007); M. C. Chen, Mod. Phys. Lett. A **21**, 621 (2006); E. Accomando *et al.*, hep-ph/0608079, Chapter 7.

[45] R. Barbieri and A. Strumia, hep-ph/0007265; Phys. Lett. B **462**, 144 (1999).

[46] N. Arkani-Hamed, A. G. Cohen, E. Katz and A. E. Nelson, JHEP **0207**, 034 (2002).

[47] C. Csaki *et al.*, Phys. Rev. D **67**, 115002 (2003); J. L. Hewett, F. J. Petriello and T. G. Rizzo, JHEP **0310**, 062 (2003).

[48] H. C. Cheng and I. Low, JHEP **0309**, 051 (2003); JHEP **0408**, 061 (2004).

[49] I. Low, JHEP **0410**, 067 (2004).

[50] J. Hubisz and P. Meade, Phys. Rev. D **71**, 035016 (2005).

[51] A. Belyaev, C. R. Chen, K. Tobe and C. P. Yuan, Phys. Rev. D **74**, 115020 (2006). *A* CalcHEP *model file for the Littlest Higgs model with T-parity*, `http://hep.pa.msu.edu/LHT/`

[52] D. Choudhury and D. K. Ghosh, JHEP **0708**, 084 (2007).

[53] J. Hubisz, P. Meade, A. Noble and M. Perelstein, JHEP **0601**, 135 (2006).

[54] J. Wess and B. Zumino, Phys. Lett. B **37**, 95 (1971); E. Witten, Nucl. Phys. B **223**, 422 (1983).

[55] C. T. Hill and R. J. Hill, Phys. Rev. D **75**, 115009 (2007); Phys. Rev. D **76**, 115014 (2007).

[56] A. Freitas, P. Schwaller and D. Wyler, JHEP **0809**, 013 (2008).

[57] A. Freitas, P. Schwaller and D. Wyler, *A* CalcHEP *model file for the Littlest Higgs model with broken T-parity*,
`http://www.itp.uzh.ch/~pedro/lht/`

[58] V. Barger, W. Y. Keung and Y. Gao, Phys. Lett. B **655**, 228 (2007).

[59] S. Mukhopadhyay, B. Mukhopadhyaya and A. Nyffeler, JHEP **1005**, 001 (2010).